Model comparisons for estimating carbon emissions from North American wildland fire

Nancy H. F. French,[1] William J. de Groot,[2] Liza K. Jenkins,[1] Brendan M. Rogers,[3] Ernesto Alvarado,[4] Brian Amiro,[5] Bernardus de Jong,[6] Scott Goetz,[7] Elizabeth Hoy,[8] Edward Hyer,[9] Robert Keane,[10] B. E. Law,[11] Donald McKenzie,[12] Steven G. McNulty,[13] Roger Ottmar,[12] Diego R. Pérez-Salicrup,[14] James Randerson,[3] Kevin M. Robertson,[15] and Merritt Turetsky[16]

Received 10 July 2010; revised 21 January 2011; accepted 10 February 2011; published 25 May 2011.

[1] Research activities focused on estimating the direct emissions of carbon from wildland fires across North America are reviewed as part of the North American Carbon Program disturbance synthesis. A comparison of methods to estimate the loss of carbon from the terrestrial biosphere to the atmosphere from wildland fires is presented. Published studies on emissions from recent and historic time periods and five specific cases are summarized, and new emissions estimates are made using contemporary methods for a set of specific fire events. Results from as many as six terrestrial models are compared. We find that methods generally produce similar results within each case, but estimates vary based on site location, vegetation (fuel) type, and fire weather. Area normalized emissions range from 0.23 kg C m^{-2} for shrubland sites in southern California/NW Mexico to as high as 6.0 kg C m^{-2} in northern conifer forests. Total emissions range from 0.23 to 1.6 Tg C for a set of 2003 fires in chaparral-dominated landscapes of California to 3.9 to 6.2 Tg C in the dense conifer forests of western Oregon. While the results from models do not always agree, variations can be attributed to differences in model assumptions and methods, including the treatment of canopy consumption and methods to account for changes in fuel moisture, one of the main drivers of variability in fire emissions. From our review and synthesis, we identify key uncertainties and areas of improvement for understanding the magnitude and spatial-temporal patterns of pyrogenic carbon emissions across North America.

Citation: French, N. H. F., et al. (2011), Model comparisons for estimating carbon emissions from North American wildland fire, *J. Geophys. Res.*, *116*, G00K05, doi:10.1029/2010JG001469.

1. Introduction

[2] Until the 1980s, when the seminal paper on carbon emissions from biomass fires by *Seiler and Crutzen* [1980] was published, the impact of fire on the balance of carbon between the land and atmosphere was thought to be unimportant. It was generally considered that while fire released carbon to the atmosphere during combustion, this carbon was then taken up by plant regrowth over a period of months to years, in many instances at a more rapid rate due to more productive conditions following the fire. This is still

[1]Michigan Tech Research Institute, Michigan Technological University, Ann Arbor, Michigan, USA.
[2]Great Lakes Forestry Research Centre, Canadian Forest Service, Sault Ste Marie, Ontario, Canada.
[3]Earth System Science Department, University of California, Irvine, California, USA.
[4]School of Forest Resources, University of Washington, Seattle, Washington, USA.
[5]Department of Soil Science, University of Manitoba, Winnipeg, Manitoba, Canada.
[6]El Colegio de la Frontera Sur, Unidad Villahermosa, Villahermosa, Tabasco, México.
[7]Woods Hole Research Center, Woods Hole, Massachusetts, USA.
[8]Department of Geography, University of Maryland, College Park, Maryland, USA.
[9]Marine Meteorology Division, Naval Research Laboratory, Monterey, California, USA.
[10]Missoula Fire Sciences Laboratory, U.S. Forest Service, Missoula, Montana, USA.
[11]College of Forestry, Oregon State University, Corvallis, Oregon, USA.
[12]Pacific Wildland Fire Sciences Laboratory, U.S. Forest Service, Seattle, Washington, USA.
[13]Eastern Forest Environmental Threat Assessment Center, U.S. Forest Service, Southern Research Station, Raleigh, North Carolina, USA.
[14]Centro de Investigaciones en Ecosistemas, Universidad Nacional Autónoma de México, Morelia, Michoacán, Campeche, México.
[15]Tall Timbers Research Station, Tallahassee, Florida, USA.
[16]Department of Integrative Biology, University of Guelph, Guelph, Ontario, Canada.

0148-0227/11/2010JG001469

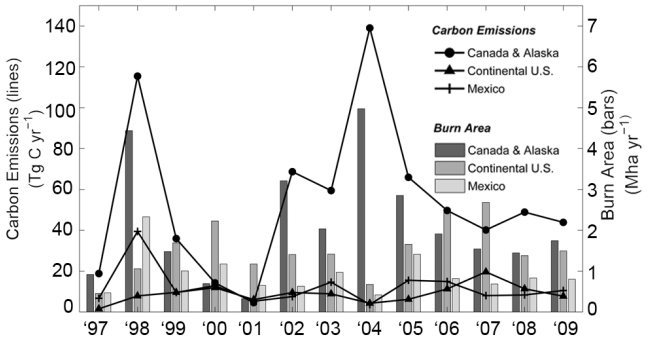

Figure 1. Annual carbon emissions (left axis) and burn area (right axis) for North American regions from the GFED3 model [*van der Werf et al.*, 2010].

the general model of disturbance and plant production except that we have learned, with more comprehensive models, that this balance is not always achieved. Changes in fire regime and land use can modify carbon cycling by several different pathways, including by altering soil microclimate and decomposition and by influencing plant species composition and thus rates of gross primary production, above ground carbon storage. Thus, the role of fire in the carbon cycle is more than just the direct addition of combusted carbon to the atmosphere during burning; fire changes the dynamics of both gross primary production and ecosystem respiration, with net ecosystem production losses continuing for several years following the event, followed by a sustained multidecadal period of net ecosystem carbon uptake [*Amiro et al.*, 2010]. Direct carbon emissions from fires are measured in a way that is fundamentally different from measurements of net ecosystem exchange (NEE) and provide an important constraint on cumulative estimates of NEE. At a global scale, direct carbon emissions from fires release 2.0 Pg yr^{-1} of carbon to the atmosphere, or about 22% of global fossil fuel emissions [*van der Werf et al.*, 2010] with important consequences for air quality, human health, and climate forcing. Our goal here is to review approaches for estimating these emissions for North America, with the aim of indentifying ways to reduce model uncertainties.

[3] Disturbance by wildland fire is common across Canada, USA, and Mexico, with most ecosystems in North America vulnerable to carbon loss through pyrogenic emissions. Wildland fires include lightning or human-caused fires (both accidental and prescribed) in forest, woodlands, shrublands, and grasslands. These fires comprise an important component of global biomass burning emissions, following the naming convention frequently used by the atmospheric science community. At a continental scale, annual emissions from North American fires vary considerably from year to year [*van der Werf et al.*, 2010] (Figure 1; also see Text S2, section S2.3, in the auxiliary material).[1] Emissions vary due to variability in the amount of burned area in different biomes from year to year as well as variability in fire severity that drives fuel consumption. Each ecoregion of North America experiences its own unique fire conditions and patterns (fire regime). In many areas the fire regime is modified through prescribed fires used for forest management and policies regulating fire suppression. The fire regime also may be changing in response to climate change [*Flannigan et al.*, 2005; *Westerling et al.*, 2006]. This is particularly evident in northern regions where warmer temperatures and longer summer season conditions have resulted in more burning in both the fire adapted boreal forests, where fire has increased [*Podur et al.*, 2002; *Kasischke et al.*, 2010] or is expected to increase with a warming climate [*Flannigan et al.*, 2005; *Amiro et al.*, 2009]. In tundra, where fires are very rare, several large and extreme events have been observed recently [*Higuera et al.*, 2008; *Racine and Jandt*, 2008]. Across North America, annual burned area has increased over the past four decades as a consequence of increasing fire activity in northern and western forests [*Gillett et al.*, 2004; *Kasischke and Turetsky*, 2006].

[4] In the boreal forest region, fire management records from Canada and a combination of fire management data and model-reconstructed burned area in Alaska [*Kasischke et al.*, 2010] show that burned area has increased between the 1950s and the end of the 20th century by 52% (from 0.49 to 0.74 Mha yr^{-1}), which means that emissions from fires in Canada and Alaska have most likely increased. In Canada, area burned increased through the 1980s and 1990s (2.7 Mha yr^{-1}) compared to the 1960s and 1970s (0.99 Mha yr^{-1}) [*Stocks et al.*, 2003; *Gillett et al.*, 2004], with area burned being a good indicator of carbon emissions [*Amiro et al.*, 2001, 2009]. However, only 17 Mha burned from 2000 to 2009 [*Canadian Interagency Forest Fire Centre*, 2010], so long-term trends are still uncertain. Much of the contemporary emissions from fires in Mexico are a result of escaped fires from agricultural burning, deforestation, and land conversion, so one can assume that biomass burning emissions in Mexico increased substantially from the 1970s onward, compared to anytime during the first part of the past century, due to increased land use. In high fire years in Mexico such as 1998, the number of wildfires almost doubled (reaching 14,445), while the total area affected more than tripled (to 850,000 ha), which illustrates how a change in weather patterns can produce extreme fire conditions. Today, total emissions from wildland fires in the conterminous United States are much lower than in the past. Based on an assessment of fire return intervals in natural ecosystems, *Leenhouts* [1998] estimated that during preindustrial times 34 to 86 Mha yr^{-1} burned in the conterminous United States releasing between 530 and 1228 Tg C yr^{-1} (1.43 to 1.56 kg C m^{-2}). By 1900, burned area in the United States decreased to 14 Mha yr^{-1}, and these fires released between 270 and 410 Tg C yr^{-1} (1.93 to 2.93 kg C m^{-2}) [*Mouillot and Field*, 2005; *Mouillot et al.*, 2006]. By the 1930s, burned area averaged 15.9 M ha yr^{-1} [*Houghton et al.*, 2000]. Based on an analysis of historical timber volume loss records from 1900 to 1990 kept by the U.S. Forest Service, we estimate forest fires in this period emitted 133 Tg C yr^{-1} (0.83 kg C m^{-2}; see Text S1). Contemporary estimates of burning within conterminous United States were 2.0 Mha yr^{-1} (during 2000–2009) and are lower than burned area estimates in boreal regions during the same period (2.5 Mha yr^{-1}), contrasting with preindustrial estimates.

[5] Past analyses show large range of emissions per unit area due in part to actual variability, from differences in fire severity and vegetation type that burned, but also due to the

[1] Auxiliary materials are available in the HTML. doi:10.1029/2010JG001469.

variable approaches and available data used to compute emissions, as is discussed further in this paper. Historically, biomass burning emissions across the entire North American continent are difficult to estimate because of a lack of consistent and reliable information on burned area, land cover, and characteristics of different fire regimes. When looking at historical emissions estimates, the reliability of the available data needs to be considered. This is especially true for data on burn area, which in some cases was based on inventories of variable quality and in other cases was modeled from information on fire return intervals or other information [e.g., *Leenhouts*, 1998].

[6] Over the past two decades, a great deal of research has been focused on developing new and more accurate information products to estimate emissions from wildland fires to help remedy inconsistencies found in past assessments. In this paper we review these terrestrial-based approaches for estimating consumption of carbon-based wildland fuels and the direct emissions of carbon from wildland fires as part of the North American Carbon Program disturbance synthesis. The purpose of this paper is to present the results of a comparison of approaches to estimating emissions from wildland fires for a set of case studies in North America and review assumptions and available areas for improvement.

2. Background

2.1. Estimating Carbon Emissions From Wildland Fires

[7] Access to a range of geospatial data in the past three decades, including information products derived from satellite remote sensing data, has improved our ability to quantify many factors relevant to the estimation of fire carbon emissions. Remote sensing provides synoptic information from the recent past and present for several important factors that are required to estimate carbon emissions, including the spatial extent of the fire, fuel characterization (fuel type, fuel load, plant physiological and moisture condition), site characteristics before and after the fire event, and environmental conditions during the fire that influence fire intensity and severity. The various approaches in use today overlap conceptually, with most using the basic framework put forth originally by *Seiler and Crutzen* [1980]. *Seiler and Crutzen* [1980] used this framework to make the first global estimates of contemporary carbon emissions from fire, separately considering emissions from different biomes and different types of land management. Application of geospatial data sets and remote sensing imagery has enhanced this basic concept.

[8] The *Seiler and Crutzen* [1980] method for estimation of carbon emissions from wildland fire requires quantification of three parameters: area burned, fuel loading (biomass per unit area), and the proportion of biomass fuel consumed, represented as fuel combustion factors and also known as the combustion completeness. The approach has been refined and emulated for studies at local, regional, and global scales for areas all over the world and a variety of timeframes [*Kasischke et al.*, 1995; *Reinhardt et al.*, 1997; *French et al.*, 2000; *Battye and Battye*, 2002; *French et al.*, 2003; *Kasischke and Bruhwiler*, 2003; *French et al.*, 2004; *Ito and Penner*, 2004; *Kasischke et al.*, 2005; *Wiedinmyer et al.*, 2006; *Campbell et al.*, 2007; *Lavoué et al.*, 2007; *Schultz et al.*, 2008; *Joint Fire Science Program*, 2009; *Ottmar et al.*, 2009; R. D. Ottmar et al., Consume 3.0, http://www.fs.fed.us/pnw/fera/research/smoke/consume/index.shtml, 2009, accessed 20 October 2010]. The general equation for computing total carbon emissions (C_t) as interpreted by *French et al.* [2002] and *Kasischke and Bruhwiler* [2003] is

$$C_t = A(Bf_c\beta) \quad (1)$$

where A is the area burned (hectares, ha or m^2), B is the biomass density or fuel load (t ha^{-1}; kg m^{-2}), f_c is the fraction of carbon in the biomass (fuel), and β is the fraction of biomass consumed in the burn.

[9] Uncertainty in emissions estimates is introduced from all of these inputs [*Peterson*, 1987; *French et al.*, 2004], and quantification of these uncertainties has been the subject of several studies, especially related to burn area [*Fraser et al.*, 2004; *Giglio et al.*, 2009; *van der Werf et al.*, 2010; *Meigs et al.*, 2011]. Some studies have used general estimates of the preburn biomass and fraction consumed, including the original *Seiler and Crutzen* [1980] approach and more recent broad-scale studies [*Schultz et al.*, 2008], but fuel consumption models are becoming increasingly more detailed, especially at finer spatial scales where data for refining emissions estimates are becoming available. The biomass or fuel load term represents all organic material at a site and is often divided into fuel components or vegetation strata because of the large differences in structure, composition, and consumption rate between fuel elements, such as trees, shrubs, grasses and sedges, coarse and fine woody debris, and surface organic material [e.g., *van der Werf et al.*, 2006; *Ottmar et al.*, 2007]. Fuel loads vary based on fuel type (a fire science term for vegetation type or ecosystem type) which can be complex in mature forest types or fairly simple in grasslands that have little to no woody debris. While fuel loading is well quantified for some ecosystems, uncertainties for others ecosystems are not well known (e.g., peatland sites and sites dominated by shrubs; see later discussion). While most emissions modeling approaches include surface organic soils as part of the fuel load, the belowground biomass held in plant roots or the organic material associated with mineral soils are not included.

[10] To derive carbon, the biomass or fuel load (*B, mass per unit area*) is multiplied by the fraction of carbon in the biomass (f_c), usually 0.45 to 0.5 for plant biomass pools and a variable fraction for surface organic materials based on the depth and level of decomposition [*French et al.*, 2003]. The β term is often called the combustion factor, combustion completeness, or burning efficiency (sometimes combustion efficiency, but we reserve this term for emissions partitioning, as explained below). The term is used to capture the variability in the material actually combusted and to determine fuel consumption (the amount of the fuel load removed during a fire). Combustion factors and fuel consumption are known to vary based on fuel type, fuel strata, and fuel condition. In many models combustion factors are determined for each fuel strata and vary due to environmental conditions, especially fuel moisture which is often included as a variable input to emissions models [*Hardy et al.*, 2001; R. D. Ottmar et al., Consume 3.0, 2009].

[11] Of the six models used in this comparison study, five of them follow the general form of equation 1. Specifics of these models are given in Text S2 and in the references

given here. The five models are (1) the First Order Fire Effects Model (FOFEM) 5.7 [*Reinhardt et al.*, 1997], (2) CONSUME 3.0 (R. D. Ottmar et al., CONSUME 3.0, 2009), (3) the newly developed Wildland Fire Emissions Information System (WFEIS), which is based on the CONSUME model [*French et al.*, 2009], (4) the Canadian Forest Service's CanFIRE 2.0 model [*de Groot*, 2010], and (5) the Global Fire Emissions Database version 3.1 (GFED3) [*van der Werf et al.*, 2010]. A related alternative to equation (1) is represented by the sixth model used in this study, the Canadian Forest Fire Behavior Prediction (FBP) System approach, which uses empirical data from controlled burns and wildfires to statistically relate fuel consumption to fuel dryness through weather parameters [*Forestry Canada Fire Danger Group*, 1992]. Application of this method is independent of biomass density, but is based on broad fuel classifications, and strong influence by weather conditions that control fuel dryness and the amount of combustion [*Amiro et al.*, 2001] (see Text S2, section S2.2.3, for background on the FBP System method).

[12] Many emissions calculations include estimation of gas and particulate components in addition to total carbon emissions. Typically, gas and particulate emissions are calculated from total fuel or carbon consumed using experimentally derived emissions factors, the ratio of a particular gas or particulate size class released to total fuel or carbon burned (e.g., g CO/kg fuel) [*Cofer et al.*, 1998; *Battye and Battye*, 2002; *Kasischke and Bruhwiler*, 2003]. To estimate the emissions of each gas species, emission factors for flaming versus smoldering (combustion stage) for each fuel component are often used to account for differences in emissions resulting from the combustion type [*Cofer et al.*, 1998; *Kasischke and Bruhwiler*, 2003]. Most of the carbon released by forest fires is in the form of carbon dioxide (CO_2, ~90% of total emissions), carbon monoxide (CO, ~9%), and methane (CH_4, ~1%) (for a review, see *Andreae and Merlet* [2001]). Many pollutants emitted from fire are products of incomplete combustion, including carbon monoxide (CO), particulate matter, and hydrocarbons. Combustion efficiency is defined as the fraction of carbon released from fuel combustion in the form of CO_2, with more "efficient" burns releasing proportionally more CO_2 than other compounds containing carbon [*Cofer et al.*, 1998]. To summarize, the composition of gaseous emissions from a fire depend not only on the amount of fuel consumed, but also on the chemical composition of the fuel and the combustion efficiency for each fuel component. For United Nations Framework Convention on Climate Change (UNFCC) purposes, CO_2 emissions from forest fires on managed lands are incorporated in estimates of ecosystem carbon stock changes, while emissions of CH_4, N_2O, and greenhouse gas precursors, including CO, are inventoried separately for forests, grasslands, and croplands as a function of the area burned, prefire carbon stocks, and fire seasonality [*National Research Council*, 2010]. Although modeling greenhouse gas emissions composition is of great interest, and has relevance for greenhouse gas inventories, air quality monitoring, and climate change policies, much of the uncertainty in these estimates arises from limits in our ability to model total biomass emissions. Here we focus our review on total carbon emissions estimates from burning, with the aim of reducing uncertainties associated with this key term.

2.2. Data Sets for Quantifying Contemporary Wildland Fire Emissions

[13] As reviewed above, the general approach for quantifying fire carbon emissions uses three basic data sets (burned area, fuel loads, and fraction of fuels consumed). The amount of prefire live and dead biomass available for burning (fuel load) and the proportion of fuel consumed (which is dependent on fuel load, fuel type, and fire weather) are difficult to measure. The high spatial and temporal variability in these factors introduces large uncertainty in wildland fire carbon emissions [*Peterson*, 1987; *Keane et al.*, 2001; *French et al.*, 2004] especially at larger than plot scales. In this section we review the methods to quantify fuel loads and fuel consumption at local to continental scales. We also discuss the assumptions underlying the quantification methods, and present results of several efforts to take the variability of these factors into account. Reviews of burned area data sets available for modeling of emissions from wildland fire in North America can be found in the literature [see, e.g., *Giglio et al.*, 2010].

2.2.1. Quantifying Fuel Loads and Fuel Consumption

[14] Wildland fire fuels are defined by the physical characteristics, such as loading (weight per unit area), size (stem or particle diameters), bulk density (weight per unit volume), and vertical and horizontal distribution of the live and dead biomass that contribute to fire behavior, fire spread, fuel consumption, and fire effects [*Keane et al.*, 2001]. Fuel loading is the quantity used in emissions modeling; it can be quantified based on field measurements or models. For woody and herbaceous low vegetation and fine and coarse dead woody debris, sampling methods range in scope from simple and rapid visual assessments to highly detailed measurements of complex fuel matrices that take considerable time and effort [for a review of field sampling methods see *Sikkink and Keane*, 2008; *Wright et al.*, 2010]. For quantifying surface organic matter (duff), techniques to measure depth of the organic layers are typically used along with some destructive sampling to quantify bulk density, and for the purposes of carbon modeling, carbon content of the various layers [*Harden et al.*, 2004; *Kasischke and Johnstone*, 2005; *Kasischke et al.*, 2008]. To estimate standing aboveground biomass fuel loads are derived from forest metrics combined with tree allometry and measured shrub biomass, which varies by species and site conditions [*Means et al.*, 1994]. The Fuel Characteristic Classification System (FCCS) [*Ottmar et al.*, 2007] and fuel loading models (FLM) [*Lutes et al.*, 2009] contain data on all these fuel strata. The FCCS provides access to a large fuel bed data library, creates and catalogs fuel beds, and classifies those fuel beds for their carbon capacity and their ability to support fire (a fuel bed is defined as the live and dead components of a site that are subject to fire [see *Riccardi et al.*, 2007b]).

[15] Model-based methods of quantifying fuels (biomass) rely on concepts from the ecological and biogeochemical modeling communities that describe the flow of carbon into and out of living biomass, litter, and woody debris pools. In the Carnegie Ames Stanford Approach (CASA) GFED3 model [*van der Werf et al.*, 2010], for example, inputs to living plant pools come from satellite-derived estimates of net primary production and plant functional type-specific patterns of allocation. Turnover rates of living biomass pools are

specified as a function of ecosystem type, with fire-induced mortality rates depending on ecosystem composition and the fire return time. Rates of litter and coarse woody debris decomposition depend on the chemical recalcitrance of the incoming plant tissue as well as temperature and soil moisture controls on the metabolism of the microbial community.

[16] Fuel consumption, referred to as combustion completeness in the GFED3 model, varies as a function of fuel type and fuel moisture (soil moisture is used within the GFED3 as a proxy model for fuel moisture status). Fuel consumption is typically quantified as an amount of the fuel load that is removed during fire. Fuel consumption (or the combustion factors that determine consumption) can be calculated from field measurements and used in models of consumption based on fuel type, fuel strata, and moisture conditions (sometimes determined from weather variables). Alternative methods to use remotely sensed information on fire severity to determine consumption have been found to be of value in some cases and not others [*French et al.*, 2008] and can be difficult to use in cases where the surface layers are strongly impacted by the fire. Similarly, fire radiative energy (FRE) measures derived from thermal infrared detectors have been shown to relate directly to fuel consumption in simple field experiments [*Wooster*, 2002]. Results using satellite data indicate that satellite-derived FRE may have some skill in capturing fuel consumption levels [*Wooster et al.*, 2005; *Ellicott et al.*, 2009]. Work remains to evaluate the range of conditions where satellite-derived FRE can be used.

[17] Empirical models of fuel consumption, including the U.S. Forest Service's CONSUME and FOFEM models and the Canadian Forest Service's FBP and CanFIRE models, have been developed largely based on experimental burns in different fuel types (for reviews, see, e.g., *Ottmar et al.* [2006] and *de Groot et al.* [2009]). These empirically derived relationships are also used to drive the fuel consumption estimates used in the GFED3 model. Controlled burns are meticulously measured before and after fire for fuel consumption data but tend to be less severe than wildfires, so this data is often combined with less rigorous, but wider-ranging wildfire data collected postfire only to improve the range of conditions used for modeling. Also, sites with deep organic soils are not well represented in controlled burns, while burning of deep organic layers in boreal forests and peatlands represent the source of most emissions in boreal regions [*Turetsky et al.*, 2011]. Because of their importance as a carbon pool, a number of studies have used sites located in natural fires [*Turetsky and Wieder*, 2001; *Benscoter and Weider*, 2003; *Harden et al.*, 2004; *Kasischke and Johnstone*, 2005; *Harden et al.*, 2006; *Kane et al.*, 2007; *de Groot et al.*, 2009] or experimentally burned natural fuels [*Benscoter et al.*, 2011] to quantify the factors controlling burning in deep organic soils. These studies have shown that although organic layer consumption is controlled in some situations by seasonal weather conditions, topography and seasonal thawing of permafrost are strong controllers of site moisture and may be equally or more important than weather for regulating the burning of deep organic layers [*Benscoter and Weider*, 2003; *Shetler et al.*, 2008].

2.2.2. Mapping Fuels for Geospatial Modeling

[18] Spatial data layers describing forest fuels are of great help in computing fuel consumption and emissions from large wildland fires. Fuel mapping, however, is a difficult and complex process requiring expertise in remotely sensed image analysis and classification, fuels modeling, ecology, geographical information systems, and knowledge-based systems. Mapping of fuel loadings can be accomplished in several ways (for a review of fuels mapping methods, see *Keane et al.* [2001] and *McKenzie et al.* [2007]), including extrapolation of field-measured fuel loads across a region, direct mapping with remote sensing, assigning loadings based on mapped fuels, empirical statistical models, or process-based simulations [*Michalek et al.*, 2000; *Keane et al.*, 2001; *McKenzie et al.*, 2007].

[19] The scale and resolution of fuel mapping depend both on objectives and availability of spatial data layers [see *McKenzie et al.*, 2007, Table 1]. For example, input layers for mechanistic fire behavior and effects models must have high resolution (<30 m [*Keane et al.*, 2000]). In contrast, continental-scale data for broad-scale assessment are usually no finer than 500 m, and often as coarse as 36 km, corresponding to the modeling domains for mesoscale meteorology and air quality assessments [*Wiedinmyer et al.*, 2006]. Many fuel mapping efforts use categories of fuel classifications rather than actual fuel loadings to accommodate the large number of fuel components and spatial variability needed to estimate carbon emissions.

[20] The high variability of fuels across time and space is a difficult obstacle to mapping of wildland fuels [*Keane et al.*, 2001; *Riccardi et al.*, 2007a; *Sikkink and Keane*, 2008]. For example, the spatial variability of fuel loading within a stand can be as high as its variability across a landscape, and this variability is different for each component [*Keane*, 2008]. In the United States, the Forest Inventory and Analysis (FIA) now measures coarse woody debris on thousands of plots, thereby improving quantification of both downed wood and aboveground live biomass [*U.S. Forest Service*, 2007]. There are also many technological challenges to mapping wildland fuels, the most important being that remotely sensed imagery used in fuels mapping is unable to detect forest surface fuels due to resolution limitations or because the ground is often obscured by the canopy. Aerial or canopy fuel loadings are somewhat easier to map directly because the loadings correlate well with vegetation classifications developed from analysis of satellite imagery and gradient modeling [*Reeves et al.*, 2009]. Work is currently underway to use new synthetic aperture radar (SAR) and lidar remote sensing systems to quantify tree canopy densities and heights and to map and model aboveground biomass. Ultimately, all remote sensing based approaches for fuels mapping need to be calibrated with in situ data. Despite the range of approaches used, the one tool that is the foundation for most mapping efforts is expert knowledge of fuels.

[21] Because of the above ecological and technological limitations, many have turned to fuel classifications for mapping of fuel biomass, rather than trying to estimate fuel quantities directly [*Nadeau et al.*, 2005; *McKenzie et al.*, 2007; *Lutes et al.*, 2009]. Fuel classifications quantify fuel loads, and therefore carbon pools, by stratifying fuel component loadings by vegetation type, biophysical setting, or fuel bed characteristics. To input fuel loading values into FOFEM, for example, *Reinhardt et al.* [1997] used the

Society of American Foresters (SAF) Cover Type Classifications by finding the mean of fuel-loading plot data within the different the SAF categories. Another example of this approach is in the mapping of FCCS fuel beds to a 1-km gridded map of the United States. FCCS mapping is two-step process of classification and quantification using a rule-based approach [*McKenzie et al.*, 2007]. An advantage of a rule-based classification is that new data layers can be incorporated efficiently because rules only need to be built for new attributes. In contrast, bringing updated data layers into model-based mapping requires entirely new models because relationships between response and predictor variables will change.

[22] Fuels maps are now or soon to be available for all areas of North America, including a map of Canadian FBP fuels for Canada [*Nadeau et al.*, 2005], two fuels maps for the United States (developed under the LANDFIRE program; http://www.landfire.gov/), and FCCS-based fuels maps in preparation for Mexico. Uncertainties are present in these maps from all the steps described above. Consequently, the accuracy and robustness of these geospatial data layers varies across North America. For example, because of fine-scale variation in fuel loadings in complex terrain, coarse-scale data (e.g., the 1 km FCCS map) may be less accurate in mountain areas than in flat topography. An unrelated source of uncertainty is the quality of inventory data used to build fuel beds or fuel models, which can vary even within a consistent protocol like the FIA. To alert users to uncertainties associated with inventory information, estimates of data quality or confidence can be added to fuel information [*Ottmar et al.*, 2007]. Robust validation of the geospatial data is nearly intractable, however, because of the scale mismatch between ground-based inventories (usually plot data) and the resolution of GIS layers.

2.3. Review of Previous Carbon Emissions Work

[23] Site-based to global-scale approaches to estimating carbon emissions from fire have been conducted in many regions and sites within North America (Table 1). In addition, there are several studies which include estimates of carbon emissions for portions of North America within a global study [e.g., *Ito and Penner*, 2004; *Schultz et al.*, 2008]. Landscape-scale research studies include a 1994 Alaskan fire [*Michalek et al.*, 2000], an assessment of black spruce in 2004 Alaska fires [*Boby et al.*, 2010], a 2002 fire in the Pacific Northwest [*Campbell et al.*, 2007], and a 2003 fire in boreal Canada [*de Groot et al.*, 2007]; the latter two are used to compare to the new case study results (Table 2). Regional assessments from the literature cover Alaska [*Kasischke and Bruhwiler*, 2003; *French et al.*, 2004, 2007], Canadian forests [*Amiro et al.*, 2001], the Canadian boreal region [*Amiro et al.*, 2009], the North American boreal region [*French et al.*, 2000; *Kasischke et al.*, 2005], and continental North America [*Wiedinmyer et al.*, 2006]. Three global studies using three different burn area data sets and modeling techniques have produced continental-scale emission estimates as well [*Hoelzemann et al.*, 2004; *Reid et al.*, 2009; *van der Werf et al.*, 2010].

[24] Estimates of carbon emissions from local-scale studies vary, as would be expected, based on vegetation type/biome and the severity of the burn, which determines the proportion consumed. The fire emissions for the Canada and Oregon fires are surprisingly similar given the differences in forest type, structure, and fire severity (1.2 to 1.9 kg C m^{-2} on average), while the Alaskan fires were somewhat higher, with emissions spanning a range of 2–5 kg C m^{-2}). The higher emissions from the black spruce fires in Alaska are at least partly caused by higher levels of consumption of organic surface fuels which are often extensive and deep within many burn perimeters [*Michalek et al.*, 2000]. Organic soils in boreal regions often can hold as much as 75% of the total fuel loading (20 kg biomass m^{-2}), according to FCCS fuel loading data [*Ottmar et al.*, 2007].

[25] The regional-scale studies of boreal North America described above, including Alaska and Canada, show a wide range of estimates that reveal key differences in modeling approaches for fuel loads and combustion factors, and thus their combined effect on fuel consumption. All of the regional-scale studies were conducted spatially, which reveals that the variability in results are a function of both the fuel loading (denser fuels in more southerly locations) and fuel consumption (a variety of fire weather conditions) [*French et al.*, 2000]. In these cases, fuel consumption was determined from a few field data sets collected by Canadian researchers studying fire effects and from research conducted in Alaska where attention was paid to improved quantification of consumption of the deep organic surface fuels during fire [*Kasischke and Bruhwiler*, 2003]. In addition to the regional-scale studies for carbon emissions, there are several activities to monitor and map emissions for air quality, which require much of the same information. In particular, the U.S. Forest Service has developed a framework for smoke modeling [*Larkin et al.*, 2009] and the NOAA Hazard Mapping System (NOAA HMS) is used to monitor and map active fire with the information available for use by NOAA and the U.S. Environmental Protection Agency (EPA) in smoke forecasting for air quality monitoring [*Rolph et al.*, 2009].

[26] Global studies of carbon emissions have concentrated on quantification of burn area, which at global scales can be the main driver of uncertainty in total emissions estimates. The GWEM study [*Hoelzemann et al.*, 2004] used the GLOBSCAR burned area product as the basis for emission estimates. Results from intercomparison of GLOBSCAR and other products [*Boschetti et al.*, 2004] indicate that this is likely to be one of the largest uncertainties in the GWEM estimates. The FLAMBE' product [*Reid et al.*, 2009] uses active fire detection products, which show a proportional response to fire activity over specific regions that is fairly reliable [*Schroeder et al.*, 2008], but exhibit dramatic variations in detection efficiency between regions. The GFED3 approach uses aggregated map of Moderate Resolution Imaging Spectroradiometer (MODIS) 500 m burned area product (the Direct Broadcast Burn Area Product (DBBAP) [*Giglio et al.*, 2009]) where available, and augments these time series with regressions with active fires to extend the global time series prior to the MODIS record [*Giglio et al.*, 2010]. GFED3 includes separate fuel loads and combustion completeness algorithms for the grass and woody vegetation components of each 0.5° grid cells, although consumption is generalized based on mean carbon pools for each of these vegetation classes at the coarse resolution of a single grid

Table 1. Input Sources and Wildland Fire Carbon Emissions Estimates From Specific Studies in North America[a]

Assessment	Description/Reference(s)	Input Source(s)			Carbon Emissions (kg C m^{-2})
		Burn Area (A)	Fuel Loading Method (B)	Fuel Consumption Method (β)	
1994 Hajdukovich Creek, Alaska	landscape-scaleAlaskan black spruce/*Michalek et al.* [2000]	remote sensing image (Landsat)	remote sensing vegetation classes with field data	remote sensing with field data	4.0 (2.8 to 8.0) kg C m^{-2}
2003 Montreal Lake fire, Saskatchewan (FBP method)	landscape-scale boreal Canada mixed conifer/*de Groot et al.* [2007]	remote sensing image (Landsat)	Canadian FBP System[b]	Canadian FBP System[b]	1.2[c] kg C m^{-2}
2003 Montreal Lake fire, Saskatchewan (BORFIRE method)	landscape-scale boreal Canada mixed conifer/*de Groot et al.* [2007]	remote sensing image (Landsat)	Canadian National Forest Inventory[d]	BORFIRE model	1.7[c] kg C m^{-2}
2002 Biscuit fire, Oregon	landscape-scale temperate mixed conifer/*Campbell et al.* [2007]	remote sensing image (Landsat)	field inventory data with remote sensing	field data with remote sensing of severity	1.9 (±0.2) kg C m^{-2}
2004 Alaska fires	landscape-scale boreal black spruce/*Boby et al.* [2010]	n/a (total emissions not calculated)	field inventory data	prefire and postfire soil and stand measures	3.3 (1.5 to 4.6) kg C m^{-2}
1950 to 1999 boreal Alaska	regional-scale Alaska boreal forest/*French et al.* [2003, 2004]	fire records	forest and soil inventory [*Kasischke et al.*, 1995]	ecoregion-level estimates from field measures	2.0 kg C m^{-2} (average for 50 years)
1959 to 1999 boreal Canada	regional-scale Canadian forest region/*Amiro et al.* [2001]	fire records	Canadian FBP System[b]	Canadian FBP System[b]	1.3 (0.9 to 2.0)[c] kg C m^{-2}
1980 to 1994 boreal North America	regional-scale boreal North America/*French et al.* [2000]	fire records	vegetation classes with field data	ecoregion-level estimates from field measures	2.1 (0.8 to 3.7) kg C m^{-2}
1992 and 1995 to 2003 boreal regions	regional-scale boreal North America/*Kasischke et al.* [2005]	fire records	forest and soil inventory [*Kasischke et al.*, 1995]	ecoregion-level estimates from field measures	1.0 to 1.8 kg C m^{-2}
1998 boreal regions	regional-scale boreal North America/*Kasischke and Bruhwiler* [2003]	fire records	ecozone-based averages from *Bourgeau-Chavez et al.* [2000]	ecozone-based averages from *French et al.* [2000]	1.4 to 2.7 kg C m^{-2}
2000 GWEM	global/*Hoelzemann et al.* [2004]	GLOBSCAR [*Simon et al.*, 2004]	LPJ-DGVM vegetation model [*Sitch et al.*, 2003]	biome mean values [*Reid et al.*, 2005]	2.7 to 4.1 kg m^{-2} (North America)
FLAMBE'	global/*Reid et al.* [2009]	FLAMBE' model[e]	FLAMBE' model[e]	FLAMBE' model[e]	2.0 to 2.3 kg m^{-2}
1997–2009 GFED	global/*van der Werf et al.* [2010]	GFED v3.1	GFED v3.1	GFED v3.1	0.20 to 9.5 kg C m^{-2} [f]

[a]Estimates and ranges reported are obtained from the publication, unless otherwise noted, and represent a variety of circumstances (e.g., range of average annual emissions or range from various regions/fuel types). Refer to individual studies for details of what the range represents. Not applicable, n/a.

[b]The Canadian FBP System models consumption as a function of fuel type and fire weather with no fuel loading determined.

[c]Study results reported as kg fuel m^{-2} shown here as kg C m^{-2} by multiplying by 0.5 g C g^{-1} dry fuel.

[d]See *de Groot et al.* [2007] and *Power and Gillis* [2006].

[e]Interannual variation, North America exagriculture.

[f]Range of averages reported by region [*van der Werf et al.*, 2010, Table 4].

Table 2. Estimates of Carbon Emitted for Case Studies[a]

Model Used (Run)	Burn Area Used in Estimate (ha)	Total Carbon Emissions (Tg C)	Area Normalized Carbon Emissions (kg C m^{-2})
Biscuit Fire			
Field-based [*Campbell et al.*, 2007]	200,000	3.80	1.9 ± 0.2
Biscuit Fire Original Fuels Map			
FOFEM 5.7[b]			
Very dry[c]	199,500[d]	8.97	4.50
Dry[c]	199,500[d]	8.26	4.14
Moderate[c]	199,500[d]	6.93	3.48
CONSUME 3.0[b]			
Very dry[c]	199,500[d]	10.62	5.32
Dry[c]	199,500[d]	9.93	4.98
Moderate[c]	199,500[d]	8.37	4.19
WFEIS[b]	200,444[d]	13.65	6.81
Biscuit Fire Revised Fuels Map			
FOFEM 5.7[e]			
Very dry[c]	199,500[d]	3.92	1.97
Dry[c]	199,500[d]	3.67	1.84
Moderate[c]	199,500[d]	3.16	1.58
CONSUME 3.0[e]			
Very dry[c]	199,500[d]	3.44	1.72
Dry[c]	199,500[d]	3.26	1.63
Moderate[c]	199,500[d]	2.63	1.32
WFEIS[e]			
Landsat burn area	200,444[d]	6.20	3.10
"Daily progression"[e]	200,154[f]	6.13	3.06
MODIS burn area[e]	169,916[g]	5.22	3.07
CanFIRE[e]	200,124[d]	3.92	1.96
FBP System[e,h]	200,124[d]	3.38	1.69
GFED	167,351[g]	3.63	2.17
Montreal Lake Fire[i]			
Canadian FBP System [*de Groot et al.*, 2007]	21,652	0.26	1.20
BORFIRE[j] [*de Groot et al.*, 2007]	21,652	0.37	1.70
FOFEM 5.7			
Very dry[c]	21,655	1.41	6.51
Dry[c]	21,655	1.27	5.88
Moderate[c]	21,655	1.03	4.76
CONSUME 3.0			
Very dry[c]	21,655	0.72	3.32
Dry[c]	21,655	0.62	2.86
Moderate[c]	21,655	0.48	2.23
CanFIRE[j]	21,652	0.44	2.32
FBP System[k]	21,652	0.17	0.79
WFEIS Landsat burn area	21,656	0.35	1.60
GFED	24,137	0.30	1.26
Boundary Fire[l]			
Field-based study (E. S. Kasischke unpublished data, 2010)	184,755[m]	4.78	2.59
FOFEM 5.7			
Very dry[c]	217,232	13.27	6.11
Dry[c]	217,232	11.99	5.52
Moderate[c]	217,232	9.71	4.47
CONSUME 3.0			
Very dry[c]	217,780	5.09	2.34
Dry[c]	217,780	4.44	2.04
Moderate[c]	217,780	3.10	1.42
CanFIRE	210,074	7.60	3.62
FBP System	210,074	2.84	1.35
WFEIS			
Landsat burn area	211,465	5.68	2.68
"Daily progression"	211,260	5.30	2.51
GFED	207,050	4.64	2.24
San Diego County October 2003[n]			
FOFEM 5.7			
Very dry[c]	143,757	1.55	1.06
Dry[c]	143,757	1.52	1.04
Moderate[c]	143,757	1.46	1.01
CONSUME 3.0			
Very dry[c]	144,657	0.77	0.53
Dry[c]	144,657	0.72	0.50
Moderate[c]	144,657	0.62	0.43
WFEIS			
Landsat burn area	150,896	1.59	1.05
"Daily progression"	150,619	1.61	1.07
GFED	100,642	0.23	0.23
San Diego County October 2007			
FOFEM 5.7			
Very dry[c]	119,565	1.26	1.08
Dry[c]	119,565	1.23	1.06
Moderate[c]	119,565	1.20	1.02
CONSUME 3.0			
Very dry[c]	122,165	0.58	0.47
Dry[c]	122,165	0.55	0.45
Moderate[c]	122,165	0.49	0.40
WFEIS			
Landsat burn area	127,381	1.28	1.01
"Daily progression"	127,347	1.31	1.03
GFED	115,476	0.40	0.35

[a]Note that the first three modeling cases listed for the Biscuit fire were done using the original version of the FCCS fuels map, while the rest of the runs used the new FCCS fuels map.
[b]Based on proportions from original 1 km FCCS map; fuel loadings range from 10.33 to 386.03 kg fuel m^{-2} (see Figure 3).
[c]See Table 3 for fuel moisture inputs used for scenarios.
[d]Landsat-derived burn area.
[e]Based on proportions from revised 1 km FCCS map; fuel loadings range from 21.37 to 860.82 kg fuel m^{-2} (see Figure 3).
[f]MODIS-derived progression burn area.
[g]MODIS-derived DBBAP burn area.
[h]Based on C-7 ponderosa pine-Douglas fir FBP System fuel type.
[i]Fuel loadings range from 6237.10 to 80,552.56 kg fuel m^{-2} (see Figure 3).
[j]BORFIRE [*de Groot et al.* 2007] and CanFIRE used the same fuel consumption algorithms for these simulations.
[k]Fuels inventory improved from *de Groot et al.* [2007].
[l]Fuel loadings range from 2614.51 to 26,397.1 kg fuel m^{-2} (see Figure 3).
[m]The Kasischke study excluded areas of cloud and cloud shadow in their Landsat-derived vegetation and burn area assessment.
[n]Fuel loadings range from 56.58 to 147,581.7 kg fuel m^{-2} (see Figure 3).

scale. This leads to important scale-dependent uncertainties that can probably only be resolved by higher spatial resolution models.

3. Methods

[27] We conducted five case study intercomparisons in a variety of locations across North America (Figure 2) to examine the assumptions, tradeoffs, and areas of uncertainty encountered in fire emissions modeling. We calculated total carbon emissions and area-normalized carbon emissions for each case using as many as six emissions models (Table 2) operating at three general spatial scales (global, regional, and local). In the analyses for the 2002 Biscuit fire, we were

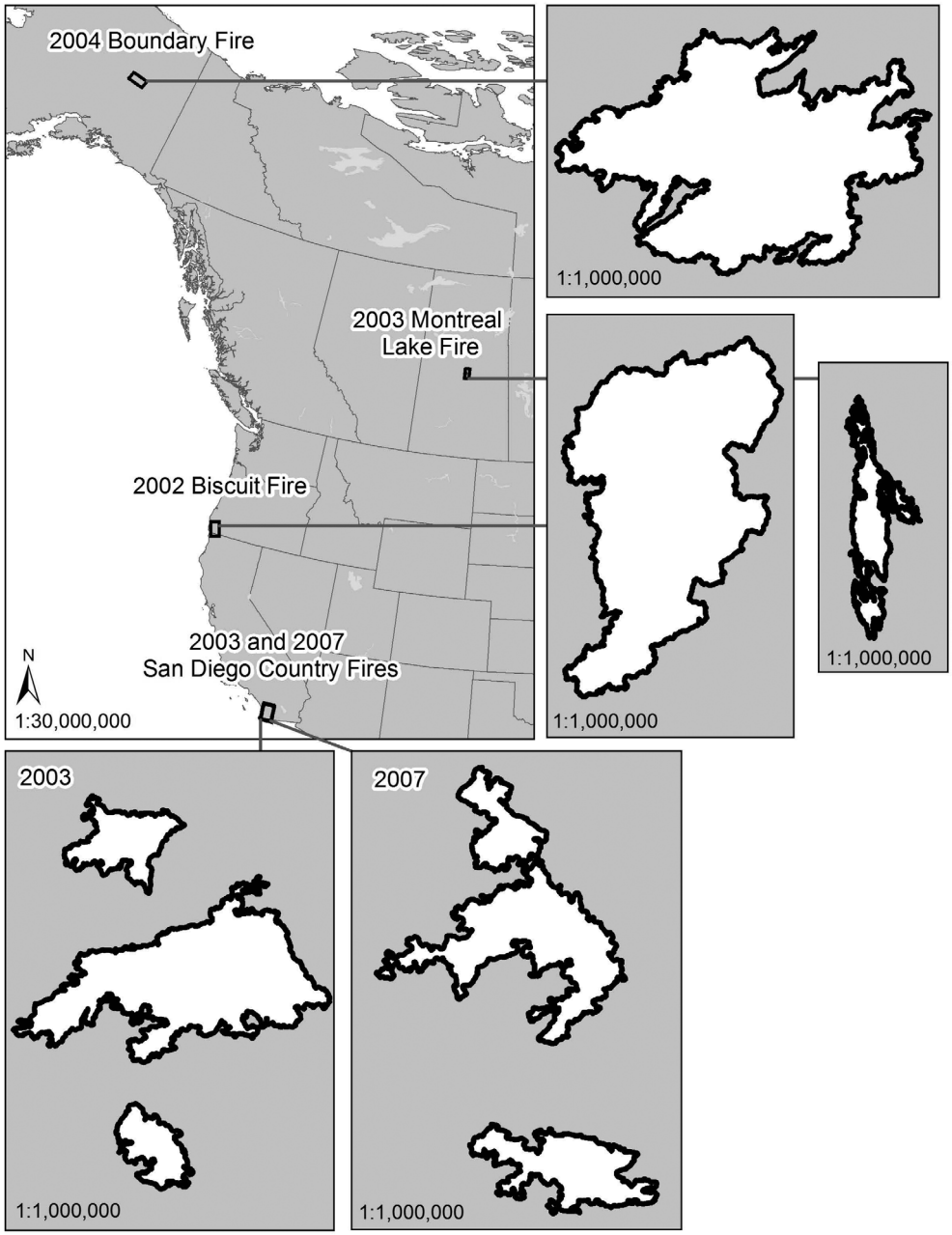

Figure 2. Location and perimeters of the five case studies.

able to vary the input data sets using several of the models to investigate the impact of variables on outcomes, including two versions of the fuel map used in some models. A full sensitivity analysis is beyond the scope of this investigation, but these model runs provide an opportunity to evaluate the range of results found with currently operating models, and develop strategies to improve the next generation of models. The studies presented represent the boreal forests of interior Alaska and west central Canada, the forests of the U.S. Pacific Northwest, and the chaparral shrublands of southern California and northern Baja California (Figure 2). In this section we review specifics of the methods used for the case studies. Results are given in Table 2 and reviewed and discussed in section 4.

3.1. Estimation of Carbon Emissions From the 2002 Biscuit Fire

[28] The Biscuit fire in SW Oregon burned approximately 200,000 ha of conifer forests in 2002. The site is dominated by Douglas fir forest communities with a ponderosa pine component (Figure 3). In a detailed study of wildland fire emissions from this event [*Campbell et al.*, 2007], federal forest inventory data with supplementary field measurements were used to estimate preburn carbon densities for 25 pools at 180 locations in the burn area. Average consumption (combustion factors) for each of these pools was compiled from the postburn assessment of thousands of individual trees, shrubs, and parcels of surface and ground fuel. The approach was based on the general equation of

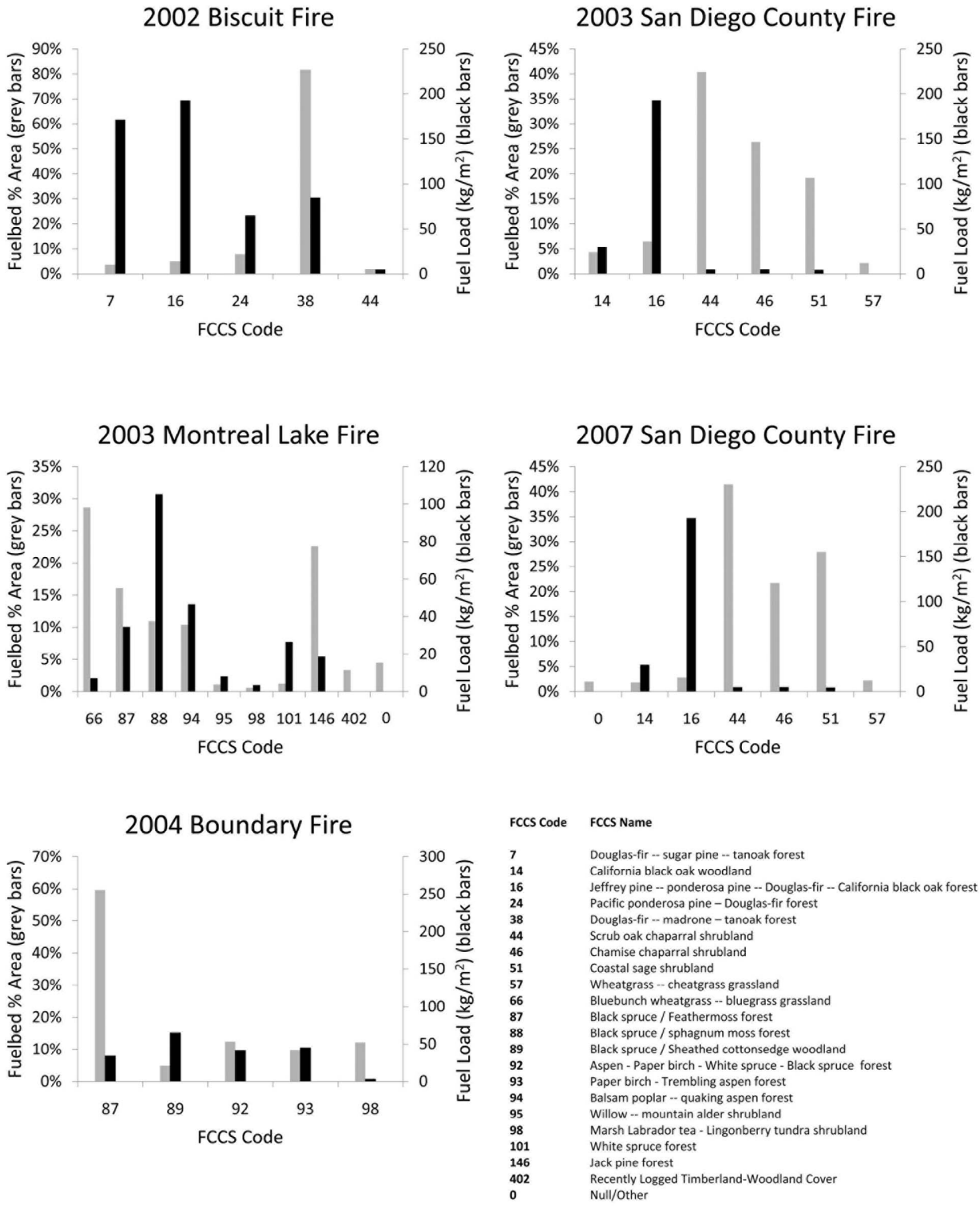

Figure 3. Graphs for each study site of the percent of each FCCS fuel bed (left axis) and total fuel loading for each fuel bed (right axis). Fuel beds are designated on the *x* axis by their FCCS codes, which are listed in the accompanying key. See http://www.fs.fed.us/pnw/fera/fccs/index.shtml for descriptions of each fuel bed.

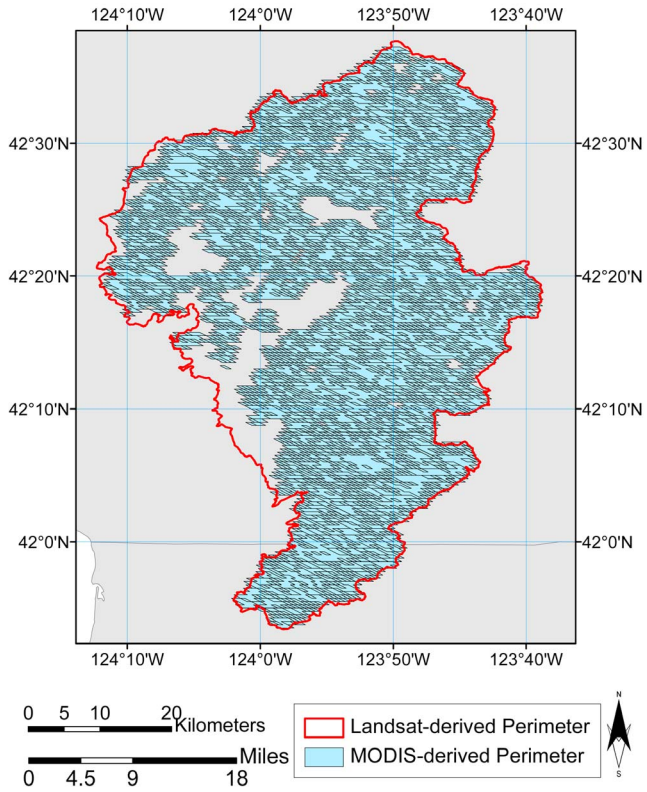

Figure 4. Burn area of the 2002 Biscuit fire in SW Oregon as mapped with Landsat (MTBS; see http://www.mtbs.gov) and with MODIS [*Giglio et al.*, 2009].

Seiler and Crutzen [1980], with the burn area partitioned by burn severity class and preburn carbon density. Four burn severities were used (high, moderate, low, and unburned/very low) and the 25 carbon pools were distinguished by vegetation tissue type, growth form, size class, and mortality status.

[29] We compared this field-based assessment to results from the CONSUME 3.0, FOFEM 5.7, CanFIRE, Canadian FBP System, WFEIS, and GFED3 models (see Text S2 for a description of these models). Data inputs varied by model, so we assessed the influence of inputs on model-dependent parameters by conducting multiple runs of some models with adjusted input data (see Table 2, Biscuit fire). Burn area for the CONSUME 3.0, FOFEM 5.7, CanFIRE, FBP System, and WFEIS runs are based on the Landsat-derived burn perimeter, which is also how the burn perimeter was determined for the field study (Figure 4 and Table 2, Biscuit fire). The burn area based on Landsat was near 200,000 ha for all variations of the Landsat-derived perimeter used by the models. An additional run of the WFEIS model was executed using the MODIS-derived 500 m resolution burn area product available in WFEIS (DBBAP [*Giglio et al.*, 2009]) to compare results when burn area source is modified. The MODIS data show the fire to have burned from 13 July to 5 September with a final size of 171,400 ha (Figure 4 and Table 2, Biscuit fire). The GFED3 estimate for this site uses a monthly 0.5° burn area map obtained by aggregating the DBBAP burn area maps.

[30] Fuel loadings for the FOFEM 5.7, CONSUME 3.0, and WFEIS runs were determined with two versions of the 1 km FCCS mapped fuel beds. One set of runs used fuel bed proportions reported by *Campbell et al.* [2007], which are derived from the original map of FCCS fuel loads [*McKenzie et al.*, 2007]. These models were also run with fuel loadings from a revised version of the 1 km FCCS map based on Landsat-derived fuel maps from the Landfire project (see http://www.fs.fed.us/pnw/fera/fccs/); this is the standard fuel bed map used in the WFEIS system. The CanFIRE model was run with the same 1 km FCCS-derived fuel loadings. The two versions of the 1 km FCCS map show very different fuel composition of the Biscuit fire. The original map, which was the map used to determine fuel proportions across the burn area in the field study, attributes about 50% of the area as western hemlock/western red cedar/Douglas fir forest and the remainder as Douglas fir dominated forest types. The revised map shows more than 80% of the area dominated by Douglas fir/madrone/tanoak forest and with no western hemlock/western red cedar/Douglas fir forest. The fuel loadings of the two types differ; based on FCCS-derived loadings the western hemlock forest holds 350 kg fuel m^{-2}, much of it in the tree bole and surface fuel layer, whereas the Douglas fir types closer to 85 kg fuel m^{-2}. The GFED3 model fuel loadings were derived within the model using CASA and satellite-derived inputs of climate and absorbed photosynthetically active radiation (see Text S2, section S2.1, for a summary of GFED3) [*van der Werf et al.*, 2010].

[31] Fuel consumption in the CONSUME 3.0, FOFEM 5.7, CanFIRE, and WFEIS models is in part determined through fuel moisture indicators, which are derived from weather-based algorithms for WFEIS and CanFIRE. For this study the CONSUME 3.0 and FOFEM 5.7 fuel moisture inputs were based on four fuel moisture scenarios included as default inputs to the FOFEM 5.7 model (shown in Table 3). WFEIS fuel moisture was determined from weather conditions on the peak day of burning, 28 July 2002, for the standard WFEIS run. The WFEIS "daily progression" estimate was based on the fire's progression across the burn area as modeled from MODIS active fire data (see, e.g., *Loboda and Csiszar* [2007] for an example of fire progression mapping), where daily fuel moisture values from 14 July to 1 September were applied to fuels burned on each day. The CanFIRE model determines fuel consumption using the Canadian Forest Fire Weather Index (FWI) System fuel moisture codes (http://cwfis.cfs.nrcan.gc.ca/en_CA/background/summary/fwi) and daily fire spread determined from the MODIS active fire product. Calculations were similar to the WFEIS "daily progression" approach where fire weather determined emissions on a daily basis, and daily emissions were summed to calculate total fire emissions.

[32] Because CanFIRE does not have any fuel models for west coast tree species, a standard conifer fuel type (jack pine) was adapted as a surrogate for the CanFIRE simulation of the Biscuit fire, which was strongly dominated by conifer species. To do this, the standard fuel components of individual stands (duff, litter, coarse woody debris, tree branch, bark, foliage, etc) within the Biscuit fire were calibrated using the spatial FCCS fuel load and height to live crown data (the revised fuel load map used in the other model

Table 3. Fuel Moisture Inputs Used for the CONSUME 3.0, FOFEM 5.7, and WFEIS Simulations[a]

	1000 h Fuel Moisture (% of Dry Weight)	Duff Fuel Moisture (% of Dry Weight)	10 h Fuel Moisture (FOFEM Only) (%)
CONSUME 3.0 and FOFEM 5.7			
Very dry	10	20	6
Dry	15	40	10
Moderate	30	75	16
Wet	40	130	22
WFEIS[b]			
Biscuit 2002	14	32	
Montreal Lake 2003	22	122	
Boundary 2004	19	27	
San Diego County 2003	7–9[c]	20	
San Diego County 2007	10–12[c]	30 to 33[c]	
CanFIRE 2.0[d]			
Biscuit 2002		20 to 44	
Montreal Lake 2003		72 to 209	
Boundary 2004		47 to 269	

[a]Other models derive fuel consumption using other inputs.
[b]Input values used for WFEIS runs with peak burn day used for modeling.
[c]The range of values for the peak burn days for the three fires modeled.
[d]Duff fuel moisture is not an input to CanFIRE but is presented for comparison purposes showing percent duff fuel moisture on the days of significant burning.

runs). The latter was necessary to ensure proper calculation of the transition from surface to crown fire modeled in CanFIRE. The FBP System estimate used the same daily approach as CanFIRE, but used the C-7 (ponderosa pine–Douglas fir) fuel type (there is no fuel load or height to live crown adjustment in FBP fuel types). Crown consumption is modeled specifically in the two Canadian models (CanFIRE and FBP System), but prescribed in a different manner in the other models. The CONSUME 3.0 and FOFEM 5.7 models are run with the default values for canopy consumption, which is zero for these models. The WFEIS model applies a canopy consumption based on the fuel bed type and the crown fire potential of that type, with fuel beds that have higher crown fire potential generally having more consumption (e.g., vegetation types that typically support crown fires have higher levels of canopy consumption).

[33] Fuel consumption in GFED3 was a function of fractional tree cover, soil moisture conditions, and carbon pool distributions. To estimate emissions for a single fire, 0.5° GFED3 output was extracted for the appropriate grid cells and months (July and August). These extractions may include additional, undesired fires in the 0.5° grid cell, although independent databases (e.g., Monitoring Trends in Burn Severity (MTBS) project) products show no other fire activity in the area.

3.2. Estimates of Carbon Emissions at the 2003 Montreal Lake Fire

[34] The Montreal Lake fire burned 21,654 ha of mixed conifer and broadleaf forest, and shrub-grasslands (Figure 3) in central Saskatchewan, Canada, over 70 days in the summer of 2003. *de Groot et al.* [2007] estimated emissions using two methods: BORFIRE, an early version of the CanFIRE model, and the Canadian FBP System method. These published BORFIRE and FBP System estimates were calculated using daily fire spread and fuels data based on a semispatial (10 km × 10 km grid) national forest inventory [*Power and Gillis*, 2006]. Similar to the Biscuit fire analysis, we compared these published results to outputs from the four other emissions models (CONSUME 3.0, FOFEM 5.7, WFEIS, and GFED3) plus two new estimates from CanFIRE and the FBP System using spatially resolved provincial forest inventory maps to determine fuel types for the FBP System simulation, and FCCS fuel beds for all other simulations.

[35] Fuel consumption was determined for each model as described for the Biscuit fire analyses, except that the WFEIS run included only the standard WFEIS approach for the peak day of burning, 19 June 2003. GFED3 was used to model emissions for June and July for the appropriate location then summed to obtain total emissions for the Montreal Lake fire event. Unlike the Biscuit fire analysis, the Montreal Lake fire study did not include a comprehensive field campaign that would permit comparison of model results to detailed ground assessments of fuel loadings and fuel consumption.

3.3. The 2004 Boundary Fire in Interior Alaska

[36] The 2004 Boundary fire, the largest fire in Alaska for 2004, started around 1 June in the hills 35 km northwest of Fairbanks and burned 217,000 ha through the month of August. The 2004 fire season was the largest in recorded history for Alaska, and the Boundary fire is representative of the type of fire that occurred in that extreme fire year. The fire burned about 60% black spruce/feather moss forest types with the remainder a mix of hardwood, spruce, and shrublands (Figure 3).

[37] We estimated emissions from the Boundary fire using the six emissions models. We compare these results to an unpublished assessment of emissions completed for the Boundary fire (E. S. Kasischke, unpublished data, 2010), which used CanFIRE fuel consumption algorithms for dead woody debris, aboveground (tree) biomass, and surface fuels (duff and litter), with the exception sites with deep organic material (black spruce and lowland sites). At these sites, detailed field data were collected to determine surface fuel loadings and consumption as a function of ecosystem type, site topography (slope, aspect, elevation), site drainage position (e.g., midslope, toe slope), and date of burn. Burn area was mapped in the Kasischke analysis with Landsat-derived perimeter and unburned interior islands resulting in 184,755 ha burn area. The 2001 National Land Cover Database (NLCD; http://landcover.usgs.gov/us_descriptions.php) map of vegetation types was used to extrapolate field-based measures of fuels and consumption across the burn, and MODIS-derived day of burning was used to determine fire weather for each location within the burn perimeter. The result of this field intensive assessment gives 4.8 Tg C of total emissions with an average emissions across the burn of 2.6 kg C m^{-2}.

[38] For the model runs fuel loadings for the area within the burn perimeter were determined for the FOFEM 5.7, CONSUME 3.0, CanFIRE, and WFEIS estimates by mapping FCCS fuel beds based on a 30 m resolution vegetation map, since the U.S. Forest Service 1 km FCCS fuel map is

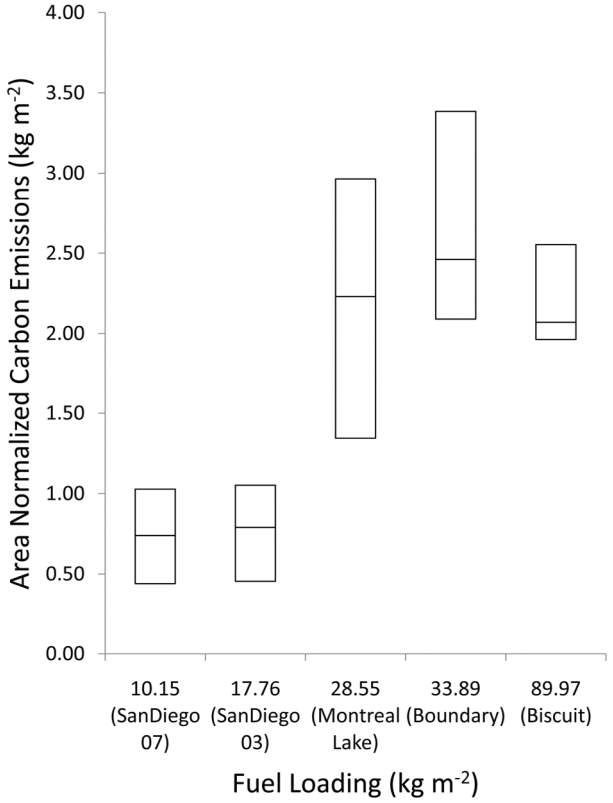

Figure 5. Box plots of median, first, and third quartiles of results from all models for the five case studies with total fuel loading for each study site shown on the *x* axis.

not yet available for Alaska. The FBP System fuel type map was derived from the FCCS fuel bed map. As with the other cases, four moisture scenarios were computed for the FOFEM 5.7 and CONSUME 3.0 runs. The WFEIS model was exercised in its standard configuration using data for 4 July 2004 to determine fuel moistures. CanFIRE and the "daily progression" WFEIS run were exercised with daily moisture data from a nearby weather station for 1 June to 30 August with fire progression determined from a MODIS active fire-derived fire progression map. GFED3 estimates were made for June, July, and August and summed for the appropriate grid cells.

3.4. Fire in Southwestern United States and Mexican Landscapes

[39] A comparison of four models was completed for fires in San Diego County, California, for two time periods from multiple fires during the major fire events of 26–29 October 2003 and 21–28 October 2007. (CanFIRE and the FBP System methods were not used because there are no shrubland fuel types in these models.) The vegetation fuel types for this case include chamise and scrub oak chaparral shrublands, coastal sage shrublands, with small components of Jeffrey pine–Ponderosa pine mixed forests and black oak woodlands (Figure 3). Fire in these vegetation types is also common in northern Baja California, Mexico, so this case is representative of a large fire-affected region of western North America.

[40] Outputs from three fires in each year were modeled and emissions combined, which together represented a large proportion of the burned area in this region for these 2 years. The 2003 analysis includes the Cedar, Paradise, and Mine-Otay fires while the 2007 analysis includes the Witch, Harris, and Poomacha fires (see, e.g., *Keeley et al.* [2004, 2009] for more information on the 2003 and 2007 San Diego fire events). For running the FOFEM 5.7, CONSUME 3.0, and WFEIS models we used fuels within the fire perimeters based on the 1 km mapped FCCS fuel beds. The GFED3 runs were analogous to the other cases. Monthly estimates for October of each year were completed for the GFED3 cells containing the fires and normalized to the combined fire area of the three fires in each year. By including a set of fires within the specified time frames we expect to capture the majority of emissions for the time and region.

4. Results and Discussion of Case Studies

[41] Results of the comparison analyses for the four case studies using six emissions models are given in Table 2 along with previous estimates for the Biscuit fire [*Campbell et al.*, 2007], Montreal Lake fire [*de Groot et al.*, 2007], and Boundary fire (E. S. Kasischke, unpublished data, 2010). Here we review these results across the sites and for each case and discuss the similarities and differences between model inputs and assumptions. The treatment of the factors that drive carbon emissions variability within the models is first discussed, followed by comparisons at each site and a discussion of model inputs and assumptions that may be contributing to the observed differences.

4.1. Comparison of Results Driven by Fuel Loading and Consumption Variability Between Sites

[42] The general trend in carbon emission among sites is predictable. Sites where fuel loads are low, such as San Diego (4.8 kg fuel m^{-2} for the dominant type: scrub oak chaparral based on FCCS; Figure 3), show lower emissions per unit area in all models (0.23 to 1.08 kg C m^{-2}; Table 2 and Figure 5) compared to the rest of the sites where fuel loads are much higher (Figure 3). Specifically, we found up to 3.10 kg C m^{-2} estimated emissions for the Biscuit fire with the revised fuel map (84.1 kg fuel m^{-2} held mainly in the canopy, bole, and dead woody debris of the Douglas fir forest which covers 82% of the burn) and up to 6.11 kg C m^{-2} emissions estimated for the Boundary fire (34.2 kg fuel m^{-2} held mainly in the duff layers of the black spruce type found in 60% of the area). Results from the Montreal Lake fire are between San Diego and these conifer sites (0.79 to 6.51 kg C m^{-2}, with most in the 1 to 3 kg C m^{-2} range), as is expected based on the mixed fuels found at this site, including a large area of grassland (29%). These trends are expected and emphasize the fact that the amount of biomass present at a site and the type of fire that is typical (e.g., crown versus surface fire) is a major driver of the variability seen in emissions across biomes beyond just accurately quantified burned area (see Table S3 in the auxiliary material). To illustrate, when looking at two cases with similar levels of burn area, San Diego 2003 and Biscuit, we see a much higher total carbon emissions from the site dominated by large conifer trees versus the shrub-dominated southwestern site no matter which model is used (Table 2).

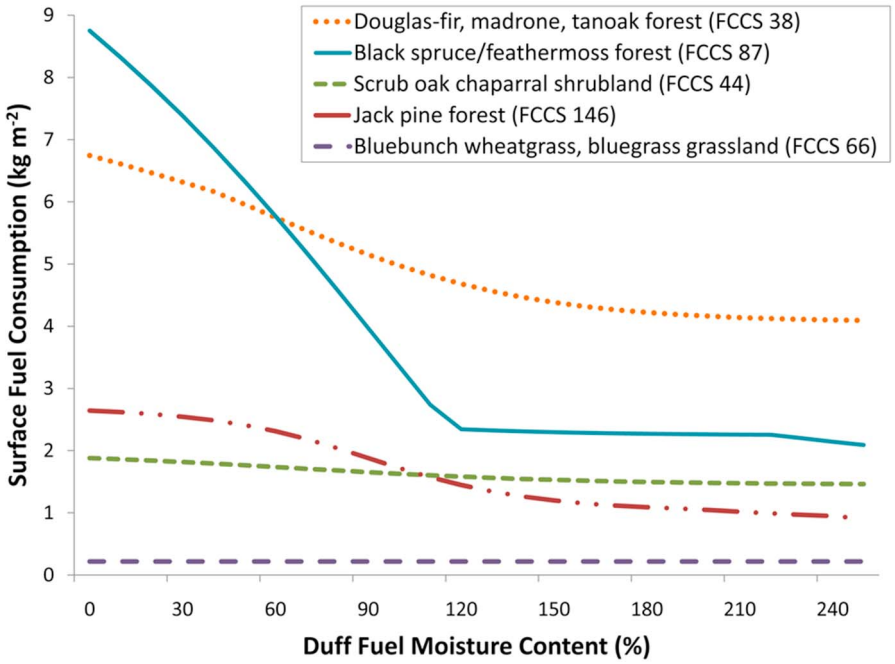

Figure 6. Relationships used in the CONSUME model between duff moisture content and total fuel consumption for five standard FCCS fuel beds. The Douglas fir type is found at the Biscuit site; the black spruce type is found at the Boundary and Montreal Lake sites. Scrub oak chaparral is found within the San Diego burns, and the jack pine and grass types are found in the Montreal Lake burn. Descriptions of these FCCS fuel beds can be found at http://www.fs.fed.us/pnw/fera/fccs/index.shtml.

[43] When moisture regime is varied, as was done with the fuel moisture scenario runs with the FOFEM 5.7 and CONSUME 3.0 models (Table 2), it is apparent that the variation from the "very dry" to "moderate" conditions is large for some sites and small for others. The Biscuit and Boundary fires show a wide range of results, whereas the results for the San Diego fires have very small variation. Looking at the moisture-consumption relationships as modeled in CONSUME (Figure 6), consumption across moisture levels does not vary nearly as greatly in the shrubland sites compared to forests because shrub types have a sharp threshold where fire will consume either all available material or none, and it is not clear how moisture drives this behavior. Shrub consumption needs more study to better determine these thresholds and moisture-consumption relationships, and this is currently being considered under a new research project being conducted by the U.S. Forest Service. The Montreal Lake results across the moisture scenarios are also less varied than the other forested sites, likely due to the large area of grassland within the burn perimeter (Figure 3).

[44] A review of the disparity in model outputs within each case shows that the FOFEM 5.7 and CONSUME 3.0 models differ in all cases, with the exception of the Biscuit fire, with FOFEM 5.7 estimating at least twice as much as CONSUME 3.0. The FOFEM 5.7 emissions estimates for the San Diego fires are roughly double those from CONSUME 3.0, and for the Boundary fire, the FOFEM 5.7 estimates are roughly triple those of CONSUME 3.0. To explain this, it should be noted that the two U.S. Forest Service models, FOFEM and CONSUME, were developed in the Pacific Northwest, so the Biscuit fire site is well represented in the parameterization of both models, and thus the model estimates for this site are similar. For the other fires, the mechanistic FOFEM model and the empirical CONSUME model produced more divergent estimates. There is an effort underway to compare CONSUME and FOFEM with a validation data set collected from 27 prescribed burns monitored for fuel consumption in pine and hardwood forest types in the eastern United States. In general, the CanFIRE model produced higher carbon emissions estimates than the Canadian FBP System, which is explained by the higher forest floor fuel consumption rate that is simulated in CanFIRE. Both of these models have empirical-based fuel consumption algorithms, but CanFIRE was developed using a larger and wider ranging forest floor data set.

[45] The choice of burn area map in estimating carbon emissions can be of consequence when calculating total carbon emissions. In the Biscuit fire case (Table 2), we ran the WFEIS model with both the Landsat-based fire progression map and the MODIS-based burn area map (DBBAP). Both maps use MODIS active fire information to define fire date, so the two products are consistent in defining the fuel consumption conditions, and the area-normalized emissions are very close (3.06 and 3.07 kg C m^{-2}). However, the total carbon emitted is higher with the Landsat-based map than with the MODIS burn area map by about 17% (6.13 Tg C with Landsat and 5.22 Tg C with MODIS) indicating that the burn area is the main driver of total emissions differences, in this case. The higher spatial resolution of the Landsat and the nature of the mapping methods used with Landsat versus MODIS, which uses an automated method to

detect burned area, means that the Landsat typically can be used to more accurately map the fire perimeter, and most often maps more burned area than the MODIS method [see, e.g., *Fraser et al.*, 2004]. The trade-off, however, is that Landsat-derived maps are not always available due to clouds and the 16 day repeat orbit, while the MODIS algorithm, which employs twice-daily imagery, allows for consistent and comprehensive mapping globally with minimal cloud interference. In addition, the MODIS-based algorithm provides a fairly accurate determination of the day of burning, not available from Landsat, and can capture unburned areas within fire perimeters often ignored in Landsat-derived perimeter maps.

4.2. Site-by-Site Comparisons of Results

[46] At the Biscuit fire site, the model runs with FOFEM 5.7, CONSUME 3.0, and WFEIS using the original version of the FCCS map (Table 2, first three models for Biscuit fire) show much higher estimates than with the revised FCCS fuel map (Table 2, remaining models for Biscuit fire), sometimes more than twice as much total carbon emissions. The driver of this is the fuel bed loading differences, as previously described. A comparison done by *Campbell et al.* [2007] of fuel loadings from their detailed estimates based on field measurements and the mapped FCCS fuel loadings (using the original FCCS map) found that when comparing fuel load values across the entire Biscuit fire, the plot-based values for surface organic material mass were lower than that of FCCS and values for litter mass were higher than that of FCCS. This discrepancy is consistent with a difference between the western hemlock/western red cedar/Douglas fir forest mapped in the original FCCS fuel map versus Douglas fir/madrone/tanoak forest in the revised FCCS fuel map. The differences found are quite possibly due to an inaccurate FCCS mapping of fuel loads, since *Campbell et al.* [2007] used the original FCCS fuel load map for the comparison.

[47] Area-normalized carbon emissions estimates for the 2002 Biscuit fire are comparable between the two nonspatial models, FOFEM 5.7 and CONSUME 3.0, using either of the fuel maps explored. The "very dry" scenarios using the revised FCCS fuel bed proportions for both models were closes to the estimate derived from field measurements. Results with revised fuel loading maps from CanFIRE, FBP System, GFED3, FOFEM 5.7, and CONSUME 3.0 are within the uncertainty estimates stated for the field-derived emissions (1.6 to 2.2 kg C m^{-2} using the "dry" or "very dry" scenarios compared to 1.9 ± 0.2 kg C m^{-2} from the field study) while the three runs of WFEIS show a higher estimated emissions of 3.1 kg C m^{-2}. With the three WFEIS model runs using the revised fuel bed map, whether the standard run, the "daily progression," or using the MODIS-derived burn area, we estimated about 50% more carbon emitted per square meter (3.06 to 3.10 kg C m^{-2}) as the field study. The fuel moistures used by WFEIS are within the range of the FOFEM 5.7 and CONSUME 3.0 ranges for "dry" to "very dry" conditions (Table 3), so the discrepancy is likely not driven by fuel moisture. The one difference that the WFEIS model includes differently from many of the other models is the consumption in the forest canopy. WFEIS prescribes canopy consumption on the basis of the fuel type and its potential to produce crown fire. The canopy consumption percent (amount of crown fuel consumed) for the fuel types within this burn range from 50 to 75%; this is likely the origin of the larger estimates by WFEIS, pointing toward a possible overestimation of canopy consumption compared to other models. This is corroborated by the CanFIRE model, which also simulates crown fire, and indicated that only about 5% of the total area burned by the Biscuit fire occurred as crown fire, a more realistic estimate.

[48] CanFIRE estimated an average emissions value (1.96 kg C m^{-2}) for the Biscuit fire case (Table 2), which was very near the field study estimate. The FBP System estimated a lower value (1.69 kg C m^{-2}). Both methods used the same daily fire spread approach with the same FWI System parameters, but there are two primary fuel-related reasons for the difference between the two Canadian emissions model results. The FBP System fuel models do not have adjustable fuel loads, whereas all fuel components can be adjusted in CanFIRE. CanFIRE can also be adjusted for height to live tree crown, which is critical for modeling crown fire, and the FBP System does not have this capability.

[49] For the Montreal Lake fire the five models have widely varying estimates (Table 2). All FOFEM 5.7 simulations produced higher estimates than all other models (4.76–6.51 kg C m^{-2}), with the CONSUME 3.0 model showing approximately half the emissions (2.23–3.32 kg C m^{-2}) of the FOFEM 5.7 model. The WFEIS model using weather data from the peak day of burning predicted 1.60 kg C m^{-2}, which is less than the CONSUME 3.0 and CanFIRE models. The low results from the WFEIS model are likely due to high duff moisture content on the day chosen to represent the burn conditions (19 June, the peak day of burn; see Table 3). Overall, the duff fuel moisture for Montreal Lake (122% for the WFEIS run) was higher than that of all other fires, but this is reasonable considering it was an early season burn, which typically means wetter surface fuel conditions than what occurs later in the season in a boreal environment. The day used for the analysis was conducive to burning, with a 1000 h fuel moisture value that fits with the dry to moderate scenario and an extreme initial spread index (ISI), which was representative of the very high fire spread rates and large area burned that day. The CanFIRE model, which included detailed information on fuels and fire progression, estimated 2.32 kg C m^{-2}, similar to the moderate moisture scenario of CONSUME 3.0. This value is higher than original estimates using the FBP System (1.20 kg C m^{-2}) and BORFIRE (1.70 kg C m^{-2}), even though all three estimates were based on a daily fire spread approach. The original BORFIRE estimate is much higher than the original FBP System estimate because the FBP System underestimates forest floor fuel consumption on deeper organic sites [*de Groot et al.*, 2007, 2009] as typically found in boreal spruce stands. Although CanFIRE and BORFIRE used the same fuel consumption algorithms, the CanFIRE estimate is higher. This is entirely related to the different forest inventory databases used to determine preburn fuel types and fuel loads. BORFIRE fuels were based on the semispatial (10 km × 10 km grid) national forest inventory (CANFI) with fuel loads calculated by the Carbon Budget Model of the Canadian Forest Sector [*Kurz et al.*, 2009]; the CanFIRE fuels were based on provincial forest inventory maps (1984 and 2003–2004 sources) with fuel loads from corresponding standard FCCS fuel beds. The wide range of results at the

Montreal Lake fire may be related to this highly variable factor which is poorly represented in the models.

[50] The fuel moisture conditions during the 2004 Boundary fire were dry (Table 3), resulting in large carbon emission estimates from some models, but not others (Table 2, Boundary fire). Both the FOFEM 5.7 and CONSUME 3.0 model scenarios show a wide range of results across the three moisture scenarios, due to the variability in the main fuel type, black spruce/feather moss, which can burn very deeply if the organic duff layer is dry (see Figure 6). In this case, much of the burning happened when the duff fuel moisture was close to the "dry" scenarios of these two models (Table 3). Again, the FOFEM results are higher than the CONSUME result, this time by a factor of three for reasons not yet understood. The CONSUME 3.0 "very dry," WFEIS (standard and daily progression), and GFED3 models are most similar (2.34, 2.68, 2.51, and 2.24 kg C m^{-2}) to the field-based estimates from E. S. Kasischke (2.59 kg C m^{-2}; unpublished data, 2010), with the CanFIRE model yielding a considerably higher estimate (3.62 kg C m^{-2}). As expected, the FBP System provided the lowest estimate due to estimation of low fuel consumption in forest floor layers. The CanFIRE model may be overestimating forest floor fuel consumption because the algorithm in that model was developed using upland sites of limited soil depth, which may not reflect higher soil moisture levels associated with deep organic soil layers in black spruce sites of interior Alaska. While GFED3 area-normalized results were within the range of the other estimates, the GFED3-derived total carbon emissions (4.64 Tg C) was lower than models which show similar area-normalized results due to the MODIS-derived burn area, which is lower than the area determined from Landsat for the other runs.

[51] For the San Diego fires, the models are all fairly similar (Table 2), although there are no field-based assessments to compare (CanFIRE and FBP System do not have shrub fuel submodels and were not used for these fires). The area-normalized results for all cases are similar, ranging from a low of 0.23 and 0.35 kg C m^{-2} from the GFED3 model for the 2003 and 2007 cases, respectively, to a high of 1.06 kg C m^{-2} for 2003 and 1.08 kg C m^{-2} for 2007 with the "very dry" FOFEM 5.7 and similar levels with the WFEIS model (1.05 and 1.02 kg C m^{-2}). In this case, the method for modeling shrub consumption is key and leads to the discrepancies found between the CONSUME 3.0 runs and WFEIS results. The WFEIS model assumed that 50% of the shrubs are consumed, whereas FOFEM 5.7 and CONSUME 3.0 were run with defaults. Using the defaults FOFEM 5.7 determined shrub consumption to be either 80% for shrub-dominated fuels and 60% for other sites and CONSUME 3.0 prescribes 0% shrub consumption as a default.

5. Discussion of Model Assumptions and Results

[52] Most of the fire emission models covered in this comparison are in an active stage of development [e.g., *de Groot*, 2010] or do not have a full uncertainty analysis available. However, model intercomparisons are often used to gain confidence in model estimates as well as to evaluate the range of uncertainty [e.g., *Friedlingstein et al.*, 2006]. For each case fire, we can estimate the variability among the models (Table 2), which to some extent, indicates the range of uncertainty if we treat each model estimate as an independent variable of equal quality. For the Biscuit fire, the mean of the six models (FOFEM revised fuel, very dry; CONSUME revised fuel, very dry; WFEIS; CanFIRE; FBP system; GFED3) is 2.27 ± 0.21 (standard error) kg C m^{-2}. The mean of the six models gives 2.16 ± 0.57 and 2.91 ± 0.61 kg C m^{-2} for the Montreal Lake (moderate scenario) and Boundary fires (dry scenario), respectively. Comparison of four models (FOFEM very dry; CONSUME very dry; WFEIS daily progression; GFED3) for the two San Diego fires each give about 0.72 ± 0.20 kg C m^{-2} with about the same percentage variability among models (20 to 25%), but a lower absolute value. This suggests that our model-to-model uncertainty ranges from ±0.2 to 0.7 kg C m^{-2}. The conclusion is that the overall uncertainty in the estimates from the ensemble of models is of the order of 25% at worst with better agreement at the Biscuit fire, although there can be a large variability among models for any given fire.

[53] Inputs to the six models were consistent with each other in many cases, but due to model construction, inputs vary from model to model producing different results. For one set of runs for the Biscuit fire, fuel loads for the FOFEM 5.7, CONSUME 3.0, CanFIRE and WFEIS simulations were determined with the same information set based on FCCS fuel beds. In the other cases, fuel loads vary due to model-determined assumptions and methods, including model scale and the use of default model-derived inputs (e.g., WFEIS uses the 1 km FCCS fuel load map and GFED3 models fuel load with a biogeochemical model). The use of fire weather data also varied widely across the six models. In this regard, all models are inherently different in some way due to assumptions, data requirements, initial model parameterization, and ability to adapt to a specific geographic region.

[54] Much of the uncertainty in estimates of carbon emissions originates in burn area uncertainty. Burn area uncertainty is associated with both the temporal aspects of the remote sensing system used to detect and map fire (such as the repeat pass timing) and the spatial resolution of remote sensing data. Variability in fire severity and unburned areas can exist within pixels and are unaccounted for in coarse resolution methods (e.g., MODIS burn area products). A published landscape analysis of remote sensing products and in situ data showed that MODIS burned area and active fire products produced omission and commission errors (missing some fire area and false identification of nonfires) when compared with Landsat burn area maps [*Meigs et al.*, 2011]. Some remote sensing products only capture canopy changes from fire, thereby missing under-canopy burning in some ecosystems. The ability of remote sensing methods to sense and accurately estimate burn area varies between biomes, and needs to be assessed with this in mind.

[55] As demonstrated from the Biscuit fire example where fuel beds were revised (first three models for Biscuit fire in Table 2 compared to remaining models for Biscuit fire in Table 2), prefire fuel loading can strongly influence carbon emission estimates. However, the Canadian FBP System fuel types do not have adjustable fuel loads, limiting the ability of the model to function properly in ecosystems that have different characteristics than those used for model calibration. On the other hand, the CanFIRE model has fully dynamic fuel models to adjust fuel type composition, loads, and physical stand structure. The FBP System and CanFIRE

are primarily based on boreal-type fuel models (with the exception of ponderosa pine–Douglas fir and coastal cedar-hemlock–Douglas fir FBP System fuel types) but there are no shrub models. Both models simulate crown fuel consumption, but CanFIRE simulates it with specific structure information. CanFIRE uses surface fire intensity and height to live crown to determine crown fire threshold (to calculate if a crown fire occurs) and has a canopy consumption algorithm, while FOFEM 5.7 and CONSUME 3.0 require user input of canopy consumption amount, and WFEIS uses fuel type-driven defaults for canopy consumption based on crown fire potential. We ran the FOFEM 5.7 and CONSUME 3.0 models with default values for this study. The software provides a way to modify the zero default, but this is user determined, so the runs done for this study were with zero canopy consumption. In the case of the Biscuit fire (and possibly other cases) this may be the reason that the CONSUME 3.0 and FOFEM 5.7 models produce lower total and per area carbon emissions than the other models that specifically model canopy consumption. WFEIS uses predetermined default inputs for canopy consumption, based on FCCS fuel bed information. Similarly, shrub consumption is treated in various ways by the different models. FOFEM 5.7 uses "rules of thumb" percent consumption values that are determined based on cover type due to a lack of adequate field data on shrub consumption. The shrub blackened input, which is the amount of area affected by fire and is an input to the CONSUME model, is always set to 50% in WFEIS. CONSUME 3.0 requires the fuel moisture, canopy consumption, and shrub blackened parameters to be loaded by the operator, and in absence of an operator decision, CONSUME 3.0 sets canopy consumption and shrub blacken to a default of 0% for both. This is unrealistic for many fuel types and fire scenario combinations, and could lead to underestimation of emissions because shrubs and the canopy are not well modeled. The zero default for shrub blackened may be the reason for lower estimates from CONSUME 3.0 at the San Diego sites, and the zero canopy consumption input may be the reason for lower estimates by CONSUME 3.0 in the Biscuit and Boundary fire cases where canopy consumption is likely not zero.

[56] Fire weather data is another source of variability between models. The FBP System and CanFIRE have fire weather-dependent fuel consumption algorithms; all simulations by those models in this study were conducted using spatial fuels data and daily fire weather to estimate daily carbon emissions as each fire spread over the landscape. For the WFEIS model we ran specialized simulations using daily spread maps for Biscuit, Boundary, and the San Diego cases ("daily progression" runs) using daily varying fuel moistures derived from weather data. The "standard" WFEIS simulations, CONSUME 3.0, and FOFEM 5.7 were run with a single set of moisture values on the peak day of burning (largest burn area). The WFEIS runs indicate that the use of a fire progression map can modify the results but in the cases shown not by very much. For the Biscuit fire the WFEIS simulation using peak fire day to represent the burn conditions was 3.10 kg C m^{-2}, and the results when the fire is run daily with the weather applied based on the fire progression was 3.06 kg C m^{-2}. It is difficult to definitively confirm that the progression-mapped WFEIS result is more accurate, but using a single day to determine burn conditions for the entire fire is not ideal, especially for long-lasting fires.

[57] The GFED3 model contains many assumptions about ecological functioning due to its structure, but generates monthly estimates of fire emissions at a global scale that are internally consistent with model estimates of net primary production and ecosystem respiration. In this way, the net ecosystem carbon balance of a region can be estimated. By dynamically modeling fuel loads as the difference between net primary production inputs and decomposition losses, GFED3 also has the advantage of allowing fuel loads to change over a period of years in response to climate warming and other drivers of global change. Results of GFED3 emissions estimates with the finer-scale models varied, with the GFED3 show lower estimates than others for the San Diego fires, but in the same range as others at Montreal Lake, Biscuit (with revised FCCS), and Boundary fires. Without quantitative uncertainty estimates for the models it is difficult to say the estimates are comparable, but the GFED3 model simulations produced estimates similar to the field-based observations (where available) indicating that the model did not have large systematic biases.

6. Conclusions and Recommendations

[58] The comparisons of carbon emissions from the five case studies using the six fire emissions models show that despite differences, these models are generally in agreement (within 25% of each other; Figure 5). Because of differences in area burned and the type, characteristics, mass, and condition of the vegetation, emissions varied between fire events for all models. Because global-scale models like GFED3 operate at coarser spatial and temporal scales, they do not capture the same degree of variability in site characteristics as do the regional-scale models, but because of the method for determining fire location and timing they can deal with time-varying factors that are important drivers for fire emissions. Our results show the global-scale model to be consistent with finer-scale methods in most cases indicating that the model includes the necessary variables for correct emissions estimation. The analyses carried out for this synthesis did not include rigorous intercomparison data (there are no uncertainty estimates nor expected range of results included with the outputs), but the analysis reveals that the models performed as expected and are appropriate candidates for further assessment.

6.1. Summary of Uncertainty Sources

[59] The variables that introduce uncertainty have been identified in past studies [*Peterson*, 1987; *French et al.*, 2004] and have helped to drive the structure of the models demonstrated here. While burn area is a known and obvious driver of total carbon emissions from fire, the magnitude of influence from fuels and fuel consumption during flaming and smoldering combustion is also of great importance in estimating trace gas and particulate emissions, but can be more difficult to quantify. The factors which introduce the most uncertainty in model estimates are the high spatial variability of fuel loadings, the fuel structure which describes how fuel loads are vertically distributed in a stand and how fire moves through a site (fire behavior), and fuel conditions at the time of the fire which is determined predominately by

weather, but also by site location (e.g., lowland versus upland) and controlled in many cases by climate variations (see discussion in Text S2, section S2.3). This study allowed a look at how different assumption on fuel loading can drive results (see the Biscuit fire example) and how ways of dealing with fuel structure can influence emissions (e.g., forest canopy consumption based on how models deal with crown fire). The study also has provided a direct look at how varying consumption based on daily burn location compares to assuming a single value for fuel moisture across an entire burn. Many past studies were not structured to account for variable fuel type, fuel loadings, and fuel conditions, but the set of models demonstrated in this study all deal with this within-burn variability in some capacity, be it by modeling several fuel types within a burn, with spatially mapped fuels, or by temporally varying conditions (daily fuel moisture).

6.2. Recommendations for Reducing Model Uncertainty

[60] Since current models have evolved to use sophisticated, detailed site/time specific information, several data sets need to be further developed to improve model estimates and to help quantify the uncertainty. Quantification and identification of the area burned is critical, and the attention being paid to improving this variable via both remote sensing and fire management records has improved the data sets immensely in the past 10 years [*Giglio et al.*, 2010]. Methods and spatial algorithms to locate and interpolate environmental data, such as weather, are also needed to take advantage of the increasing access to remote sensing products that can provide information on daily fire location. Weather data are needed to estimate fuel moisture, which in turn controls biomass consumption as well as the rate of fire spread. Data at finer temporal and spatial scales can only increase the accuracy of model estimates; but environmental data sets are not always available for some regions at useful scales (landscape to subregional). For example, weather stations in Alaska and Mexico are much more dispersed than is needed to properly map weather-derived fuel moisture variables.

[61] To determine combustion factors for different pools and burn severities, more field collected data is needed from various forest and vegetation types, different climate zones, and under different burning conditions. Prefire and postfire measurements covering many North American fuel types are needed including dead woody debris, litter, duff, and soil organic material for a range of tree size classes. For all models, the most serious problem in estimating carbon emissions in northern forests is the lack of a widely applicable fuel consumption model for deep organic soils, peatlands, and heavy accumulations of large fuels (e.g., slash piles, wind-blown timber) [*Benscoter et al.*, 2011]. Field studies and data sets to properly quantify fuels and consumption in tropical and subtropical locations are not as extensive as for temperate regions. Mapped fuels data are difficult to obtain for regions of Mexico, but data to inform maps may become available soon because in 2009 fuel load measurements were incorporated into national forest inventory protocols.

[62] For all regions, fuel loadings in shrub types are not well quantified, and shrub-dominated landscapes are not well modeled for fire effects, including fuel consumption. Although field assessment have been made in some areas, this information has not been integrated with the models demonstrated in this study. Further work for the FCCS system and the CONSUME model will lead to improvements in how to quantify shrub fuel loads and consumption. Additional fuel models are being developed for CanFIRE, and the consumption of canopy and shrub components must be improved for the BURNUP model in FOFEM so that the method can be more robustly ported across ecosystems. Conversion of live to dead biomass after fire is difficult to estimate and many models simply assume a fixed fraction across a broad range of conditions. Uncertainty in spatial estimates of live biomass can be reduced in the future with new remote sensing systems, such as synthetic aperture radar and lidar, which are sensitive to canopy volume and forest structure. Attention to data gaps in fuel condition will substantially improve emissions estimates in regions where fire can or may be of great importance, such as peatland and permafrost regions of the north where climate warming trends portend increased fire [*Flannigan et al.*, 2005]. Finally, while approaches to use satellite imagery to estimate burn severity are being developed, few studies have been able to directly link the satellite approaches for estimation of fuel consumption [*Wooster et al.*, 2005; *French et al.*, 2008].

[63] As discussed earlier, the scale of the emissions model dictates the model structure, parameterization, and available input data, so improvements in fuel (biomass) characterization and the state of the fuels during fire (e.g., structure and moisture) will depend on the level of spatial detail expected. If variability in inputs cannot be accommodated, due to lack of data or limitations of the model (intended or not), the variability needs to be represented as an uncertainty that is properly quantified within the model. One of the next steps in the process of building effective means of quantifying emissions at multiple scales is to conduct rigorous model intercomparison studies, where a few (2 or 3) models are all exercised with constant input data sets, and model uncertainly is computed. Only then will the true "validity" of these models be revealed and specific improvement points for each model identified.

[64] Further testing of the mechanistic models, such as FOFEM and GFED3 in fuel types not yet investigated is warranted. Similarly, empirical models and empirical data sets used to build the process-based models require more data sets, as stated above. The inconsistencies demonstrated in the comparisons shown between FOFEM 5.7 and CONSUME 3.0 point to the lack of testing in sites outside of the region where the models were developed. Improved relationships derived from field-based and remote sensing measurements can only improve these models. A stellar example of this need for extended model development and site-based model assessments for modeling fire effects, including emissions, is northern peatlands, where carbon pools are large and carbon loss from fire can be exceptional [*Turetsky et al.*, 2002].

[65] The review of models presented indicates that an impressive amount of effort has been put toward understanding pyrogenic carbon emissions, a factor considered of little importance only three decades ago, and poorly quantified until these past few years. The results of the case studies also show, however, that there are inconsistencies in the estimates of carbon emissions from fire, and that various models are not in agreement on how to make the best esti-

mate. Scale, as previously mentioned, is to be considered, as a global understanding of fire's role in carbon cycle requires different assumptions than a landscape or regional-scale understanding. The study we have presented helps frame the set of issues involved, and provides a review of the data sets that need improvement if accurate estimates of pyrogenic emissions are to be made across all regions.

[66] **Acknowledgments.** The authors would like to acknowledge the work of Marlene Tyner and Benjamin Koziol at MTRI and Alan Cantin at CFS for their contributions in model calculation activities. Also, we would like to acknowledge the assistance of E. S. Kasischke for his suggestions and editing of a previous version of this manuscript. N.H.F. French and L. K. Jenkins were supported on this project by NASA grant NNX08AK69G from the Applied Sciences and Carbon Cycle Science programs. NASA also provided support for the development of the GFED3 fire emissions estimates described here.

References

Amiro, B. D., J. B. Todd, B. M. Wotton, K. A. Logan, M. D. Flannigan, B. J. Stocks, J. A. Mason, D. L. Martell, and K. G. Hirsch (2001), Direct carbon emissions from Canadian forest fires, 1959–1999, *Can. J. For. Res.*, *31*, 512–525, doi:10.1139/cjfr-31-3-512.

Amiro, B. D., A. Cantin, M. D. Flannigan, and W. J. de Groot (2009), Future emissions from Canadian boreal forest fires, *Can. J. For. Res.*, *39*, 383–395, doi:10.1139/X08-154.

Amiro, B. D., et al. (2010), Ecosystem carbon dioxide fluxes after disturbance in forests of North America, *J. Geophys. Res.*, *115*, G00K02, doi:10.1029/2010JG001390.

Andreae, M. O., and P. Merlet (2001), Emission of trace gases and aerosols from biomass burning, *Global Biogeochem. Cycles*, *15*(4), 955–966, doi:10.1029/2000GB001382.

Battye, W. B., and R. Battye (2002), Development of emissions inventory methods for wildland fire, final report, U.S. Environ. Protect. Agency, Research Triangle Park, N. C. (Available at http://www.epa.gov/ttn/chief/ap42/ch13/related/firerept.pdf, accessed 15 Oct. 2008.)

Benscoter, B. W., and R. K. Weider (2003), Variability in organic matter lost by combustion in a boreal bog during the 2001 Chisholm fire, *Can. J. For. Res.*, *33*, 2509–2513, doi:10.1139/x03-162.

Benscoter, B. W., D. K. Thompson, J. M. Waddington, M. D. Flannigan, B. M. Wotton, W. J. de Groot, and M. R. Turetsky (2011), Interactive effects of vegetation, soil moisture, and bulk density on depth of burning of thick organic soils, *Int. J. Wildland Fire*, in press.

Boby, L. A., E. A. Schuur, M. C. Mack, D. Verbyla, and J. F. Johnstone (2010), Quantifying fire severity, carbon, and nitrogen emissions in Alaska's boreal forest, *Ecol. Appl.*, *20*(6), 1633–1647, doi:10.1890/08-2295.1.

Boschetti, L., H. D. Eva, P. A. Brivio, and J. M. Grégoire (2004), Lessons to be learned from the comparison of three satellite-derived biomass burning products, *Geophys. Res. Lett.*, *31*, L21501, doi:10.1029/2004GL021229.

Bourgeau-Chavez, L. L., E. S. Kasischke, J. P. Mudd, and N. H. F. French (2000), Characteristics of forest ecozones in the North American boreal region, in *Fire, Climate Change, and Carbon Cycling in the North American Boreal Forest*, edited by E. S. Kasischke and B. J. Stocks, pp. 258–273, Springer, New York.

Campbell, J., D. Donato, D. Azuma, and B. Law (2007), Pyrogenic carbon emission from a large wildfire in Oregon, United States, *J. Geophys. Res.*, *112*, G04014, doi:10.1029/2007JG000451.

Canadian Interagency Forest Fire Centre (2010), Annual fire reports, Winnipeg, Manit., Canada. (Available at http://www.ciffc.ca/, accessed 30 Sept. 2010.)

Cofer, W. R., III, E. L. Winstead, B. J. Stocks, J. G. Goldammer, and D. R. Cahoon (1998), Crown fire emissions of CO_2, CO, H_2, CH_4 and TNMHC from a dense jack pine boreal forest fire, *Geophys. Res. Lett.*, *25*, 3919–3922, doi:10.1029/1998GL900042.

de Groot, W. J. (2010), Modeling fire effects: Integrating fire behaviour and fire ecology, paper presented at 6th International Conference on Forest Fire Research, ADAI/CEIF Univ. of Coimbra, Coimbra, Portugal, 15–18 Nov.

de Groot, W. J., et al. (2007), Estimating direct carbon emissions from Canadian wildland fires, *Int. J. Wildland Fire*, *16*, 593–606, doi:10.1071/WF06150.

de Groot, W. J., J. Pritchard, and T. J. Lynham (2009), Forest floor fuel consumption and carbon emissions in Canadian boreal forest fires, *Can. J. For. Res.*, *39*, 367–382, doi:10.1139/X08-192.

Ellicott, E., E. Vermote, L. Giglio, and G. Roberts (2009), Estimating biomass consumed from fire using MODIS FRE, *Geophys. Res. Lett.*, *36*, L13401, doi:10.1029/2009GL038581.

Flannigan, M. D., K. A. Logan, B. D. Amiro, and W. R. Skinner (2005), Future area burned in Canada, *Clim. Change*, *72*, 1–16, doi:10.1007/s10584-005-5935-y.

Forestry Canada Fire Danger Group (1992), Development and structure of the Canadian Forest Fire Behavior Prediction System, *Rep. ST-X-3*, Forest. Can., Ottawa, Ont.

Fraser, R. H., R. J. Hall, R. Landry, T. J. Lynham, D. Raymond, B. Lee, and Z. Li (2004), Validation and calibration of Canada-wide coarse-resolution satellite burned-area maps, *Photogramm. Eng. Remote Sens.*, *70*(4), 451–460.

French, N. H. F., E. S. Kasischke, B. J. Stocks, J. P. Mudd, D. L. Martell, and B. S. Lee (2000), Carbon release from fires in the North American boreal forest, in *Fire, Climate Change, and Carbon Cycling in the Boreal Forest*, edited by E. S. Kasischke and B. J. Stocks, pp. 377–388, Springer, New York.

French, N. H. F., E. S. Kasischke, J. E. Colwell, J. P. Mudd, and S. Chambers (2002), Preliminary assessment of the impact of fire on surface albedo, in *Proceedings of IBFRA 2000 Conference, May 8–12, 2000, Edmonton, Alberta, Canada*, edited by C. H. Shaw and M. J. Apps, pp. 41–52, North. For. Cent., Can. For. Serv., Edmonton, Alberta, Canada.

French, N. H. F., E. S. Kasischke, and D. G. Williams (2003), Variability in the emission of carbon-based trace gases from wildfire in the Alaskan boreal forest, *J. Geophys. Res.*, *108*(D1), 8151, doi:10.1029/2001JD000480].

French, N. H. F., P. Goovaerts, and E. S. Kasischke (2004), Uncertainty in estimating carbon emissions from boreal forest fires, *J. Geophys. Res.*, *109*, D14S08, doi:10.1029/2003JD003635.

French, N. H., B. W. Koziol, R. B. Powell, and L. Spaete (2007), Variability in fuel consumption across fire-effected boreal and western North American forest regions, *Eos Trans. AGU*, *88*(52), Fall Meet. Suppl., Abstract B14C-06.

French, N. H. F., E. S. Kasischke, R. J. Hall, K. A. Murphy, D. L. Verbyla, E. E. Hoy, and J. L. Allen (2008), Using Landsat data to assess fire and burn severity in the North American boreal forest region: An overview and summary of results, *Int. J. Wildland Fire*, *17*(4), 443–462, doi:10.1071/WF08007.

French, N. H. F., T. A. Erickson, D. McKenzie, M. Billmire, and C. Hatt (2009), The Wildland Fire Emissions Information System: Providing information for carbon cycle studies with open source GIS tools, paper presented at North American Carbon Program—2nd All-Investigators Meeting, San Diego, Calif., Feb.

Friedlingstein, P., et al. (2006), Climate-carbon cycle feedback analysis: Results from the C4 MIP model intercomparison, *J. Clim.*, *19*(14), 3337–3353, doi:10.1175/JCLI3800.1.

Giglio, L., T. Loboda, D. P. Roy, B. Quayle, and C. O. Justice (2009), An active-fire based burned area mapping algorithm for the MODIS sensor, *Remote Sens. Environ.*, *113*(2), 408–420, doi:10.1016/j.rse.2008.10.006.

Giglio, L., J. T. Randerson, G. R. van der Werf, P. S. Kasibhatla, G. J. Collatz, D. C. Morton, and R. S. DeFries (2010), Assessing variability and long-term trends in burned area by merging multiple satellite fire products, *Biogeosciences*, *7*, 1171–1186, doi:10.5194/bg-7-1171-2010.

Gillett, N. P., A. J. Weaver, F. W. Zwiers, and M. D. Flannigan (2004), Detecting the effect of climate change on Canadian forest fires, *Geophys. Res. Lett.*, *31*, L18211, doi:10.1029/2004GL020876.

Harden, J. W., J. C. Neff, D. V. Sandberg, M. R. Turetsky, R. Ottmar, G. Gleixner, T. L. Fries, and K. L. Manies (2004), Chemistry of burning the forest floor during the FROSTFIRE experimental burn, interior Alaska, 1999, *Global Biogeochem. Cycles*, *18*, GB3014, doi:10.1029/2003GB002194.

Harden, J. W., K. L. Manies, M. R. Turetsky, and J. C. Neff (2006), Effects of wildfire and permafrost on soil organic matter and soil climate in interior Alaska, *Global Change Biol.*, *12*, 2391–2403, doi:10.1111/j.1365-2486.2006.01255.x.

Hardy, C. C., R. D. Ottmar, J. L. Peterson, J. E. Core, and P. Seamon (2001), *Smoke management guide for prescribed and wildland fire: 2001 edition*. *PMS 420–2*, 226 pp., National Wildfire Coordination Group, Boise, Idaho.

Higuera, P. E., L. B. Brubaker, P. M. Anderson, T. A. Brown, A. T. Kennedy, and F. S. Hu (2008), Frequent fires in ancient shrub tundra: Implications of paleorecords for arctic environmental change, *PLoS ONE*, *3*(3), e0001744, doi:10.1371/journal.pone.0001744.

Hoelzemann, J. J., M. G. Schultz, G. P. Brasseur, C. Granier, and M. Simon (2004), Global Wildland Fire Emission Model (GWEM): Evaluating the use of global area burnt satellite data, *J. Geophys. Res.*, *109*, D14S04, doi:10.1029/2003JD003666.

Houghton, R. A., J. L. Hackler, and K. T. Lawrence (2000), Changes in terrestrial carbon storage in the United States. 2: The role of fire and fire management, *Global Ecol. Biogeogr.*, *9*(2), 145–170, doi:10.1046/j.1365-2699.2000.00164.x.

Ito, A., and J. E. Penner (2004), Global estimates of biomass burning emissions based on satellite imagery for the year 2000, *J. Geophys. Res.*, *109*, D14S05, doi:10.1029/2003JD004423.

Joint Fire Science Program (2009), Consume 3.0—A software tool for computing fuel consumption, *Fire Sci. Brief*, *66*(June 2009), 6 pp.

Kane, E. S., E. S. Kasischke, D. W. Valentine, M. R. Turetsky, and A. D. McGuire (2007), Topographic influences on wildfire consumption of soil organic carbon in black spruce forests of interior Alaska: Implications for black carbon accumulation, *J. Geophys. Res.*, *112*, G03017, doi:10.1029/2007JG000458.

Kasischke, E. S., and L. M. Bruhwiler (2003), Emissions of carbon dioxide, carbon monoxide and methane from boreal forest fires in 1998, *J. Geophys. Res.*, *108*(D1), 8146, doi:10.1029/2001JD000461.

Kasischke, E. S., and J. F. Johnstone (2005), Variation in postfire organic layer thickness in a black spruce forest complex in Interior Alaska and its effects on soil temperature and moisture, *Can. J. For. Res.*, *35*, 2164–2177, doi:10.1139/x05-159.

Kasischke, E. S., and M. R. Turetsky (2006), Recent changes in the fire regime across the North American boreal region: Spatial and temporal patterns of burning across Canada and Alaska, *Geophys. Res. Lett.*, *33*, L09703, doi:10.1029/2006GL025677.

Kasischke, E. S., N. H. F. French, L. L. Bourgeau-Chavez, and N. L. Christensen Jr. (1995), Estimating release of carbon from 1990 and 1991 forest fires in Alaska, *J. Geophys. Res.*, *100*(D2), 2941–2951, doi:10.1029/94JD02957.

Kasischke, E. S., E. J. Hyer, P. C. Novelli, L. P. Bruhwiler, N. H. F. French, A. I. Sukhinin, J. H. Hewson, and B. J. Stocks (2005), Influences of boreal fire emissions on Northern Hemisphere atmospheric carbon and carbon monoxide, *Global Biogeochem. Cycles*, *19*, GB1012, doi:10.1029/2004GB002300.

Kasischke, E. S., M. R. Turetsky, R. D. Ottmar, N. H. F. French, G. Shetler, E. Hoy, and E. S. Kane (2008), Evaluation of the composite burn index for assessing fire severity in black spruce forests, *Int. J. Wildland Fire*, *17*(4), 515–526, doi:10.1071/WF08002.

Kasischke, E. S., et al. (2010), Alaska's changing fire regime - implications for the vulnerability of its boreal forests, *Can. J. For. Res.*, *40*(7), 1313–1324, doi:10.1139/X10-098.

Keane, R. E. (2008), Biophysical controls on surface fuel litterfall and decomposition in the northern Rocky Mountains, USA, *Can. J. For. Res.*, *38*, 1431–1445, doi:10.1139/X08-003.

Keane, R. E., S. A. Mince-Moyer, K. M. Schmidt, D. G. Long, and J. L. Garner (2000), Mapping vegetation and fuels for fire management on the Gila national forest complex, New Mexico, *Gen. Tech. Rep. RMRS-46-CD*, U.S. For. Serv., U.S. Dep. of Agric., Washington, D. C.

Keane, R. E., R. E. Burgan, and J. W. Van Wagtendonk (2001), Mapping wildland fuels for fire management across multiple scales: Integrating remote sensing, GIS, and biophysical modeling, *Int. J. Wildland Fire*, *10*, 301–319, doi:10.1071/WF01028.

Keeley, J. E., C. J. Fotheringham, and M. A. Mority (2004), Lessons from the October 2003 wildfires in Southern California, *J. For.*, *102*, 26–31.

Keeley, J. E., H. Safford, C. J. Fotheringham, J. Franklin, and M. Moritz (2009), The 2007 Southern California wildfires: Lessons in complexity, *J. For.*, *107*(6), 287–296.

Kurz, W. A., et al. (2009), CBM-CFS3: A model of carbon-dynamics in forestry and land-use change implementing IPCC standards, *Ecol. Modell.*, *220*(4), 480–504, doi:10.1016/j.ecolmodel.2008.10.018.

Larkin, N. K., S. M. O'Neill, R. Solomon, S. Raffuse, T. Strand, D. C. Sullivan, C. Krull, M. Rorig, J. Peterson, and S. A. Ferguson (2009), The BlueSky smoke modeling framework, *Int. J. Wildland Fire*, *18*(8), 906–920, doi:10.1071/WF07086.

Lavoué, D., S. Gong, and B. J. Stocks (2007), Modeling of emissions from Canadian wildfires: A case study of the 2002 Quebec fires, *Int. J. Wildland Fire*, *16*, 649–663, doi:10.1071/WF06091.

Leenhouts, B. (1998), Assessment of biomass burning in the conterminous United States, *Ecol. Soc.* [online], *2*(1). (Available at http://www.consecol.org/vol2/iss1/art1/, accessed 21 Jan. 2011.)

Loboda, T., and I. Csiszar (2007), Reconstruction of fire spread within wildland fire events in northern Eurasia from the MODIS active fire product, *Global Planet. Change*, *56*(3–4), 258–273, doi:10.1016/j.gloplacha.2006.07.015.

Lutes, D. C., R. E. Keane, and J. F. Caratti (2009), A surface fuels classification for estimating fire effects, *Int. J. Wildland Fire*, *18*, 802–814, doi:10.1071/WF08062.

McKenzie, D., C. L. Raymond, L.-K. B. Kellogg, R. A. Norheim, A. G. Andreu, A. C. Bayard, K. E. Kopper, and E. Elman (2007), Mapping fuels at multiple scales: Landscape application of the Fuel Characteristic Classification System, *Can. J. For. Res.*, *37*, 2421–2437, doi:10.1139/X07-056.

Means, J. E., H. A. Hansen, G. J. Koerper, P. B. Alaback, and M. W. Klopsch (1994), Software for computing plant biomass—BIOPAK users guide, *Gen. Tech. Rep. PNW-GTR-340*, 184 pp., Pac. Northwest Res. Stn., U.S. For. Serv., U.S. Dep. of Agric., Portland, Oreg.

Meigs, G. W., D. P. Turner, W. D. Ritts, Y. Zhiqiang, and B. E. Law (2011), Detection and simulation of heterogeneous fire effects on pyrogenic emissions, tree mortality, and net ecosystem production, *Ecosystems*, in press.

Michalek, J. L., N. H. F. French, E. S. Kasischke, R. D. Johnson, and J. E. Colwell (2000), Using Landsat TM data to estimate carbon release from burned biomass in an Alaskan spruce complex, *Int. J. Remote Sens.*, *21*(2), 323–338, doi:10.1080/014311600210858.

Mouillot, F., and C. B. Field (2005), Fire history and the global carbon budget: A 1 degrees x 1 degrees fire history reconstruction for the 20th century, *Global Change Biol.*, *11*, 398–420, doi:10.1111/j.1365-2486.2005.00920.x.

Mouillot, F., A. Narasimha, Y. Balkanski, J. F. Lamarque, and C. B. Field (2006), Global carbon emissions from biomass burning in the 20th century, *Geophys. Res. Lett.*, *33*, L01801, doi:10.1029/2005GL024707.

Nadeau, L. B., D. J. McRae, and J.-Z. Jin (2005), Development of a national fuel-type map for Canada using fuzzy logic, *Inf. Rep. NOR-X-406*, 17 pp., Can. For. Serv., Ottawa.

National Research Council (2010), *Verifying Greenhouse Gas Emissions: Methods to Support International Climate Agreements*, Natl. Acad. Press, Washington, D. C.

Ottmar, R. D., S. J. Pritchard, R. E. Vihnanek, and D. V. Sandberg (2006), Modification and validation of fuel consumption models for shrub and forested lands in the southwest, Pacific Northwest, Rockies, Midwest, southeast and Alaska, *Final Report JFSP Project 98-1-9-06*, 14 pp., publisher, location.

Ottmar, R. D., D. V. Sandberg, C. L. Riccardi, and S. J. Prichard (2007), An overview of the Fuel Characteristic Classification System (FCCS)—Quantifying, classifying, and creating fuelbeds for resource planning, *Can. J. For. Res.*, *37*, 2383–2393, doi:10.1139/X07-077.

Ottmar, R. D., A. Miranda, and D. Sandberg (2009), Characterizing sources of emissions from wildland fires, in *Wildland Fires and Air Pollution*, edited by A. Bytnerowicz et al., pp. 61–78, Elsevier, Amsterdam.

Peterson, J. L. (1987), Analysis and reduction of the errors of predicting prescribed burn emissions, Master's thesis, 70 pp., Univ. of Wash., Seattle.

Podur, J., D. L. Martell, and K. Knight (2002), Statistical quality control analysis of forest fire activity in Canada, *Can. J. For. Res.*, *32*, 195–205, doi:10.1139/x01-183.

Power, K., and M. D. Gillis (2006), Canada's forest inventory 2001, *Inf. Rep. BCX-408E*, Nat. Resour. Can., Can. For. Serv., Victoria, B. C.

Racine, C., and R. Jandt (2008), The 2007 'Anaktuvuk River' tundra fire on the Arctic Slope of Alaska: A new phenomenon?, paper presented at Ninth International Conference on Permafrost, U.S. Permafrost Assoc., Fairbanks, Alaska, 29 June to 3 July.

Reeves, M. C., K. C. Ryan, M. C. Rollins, and T. G. Thompson (2009), Spatial fuel data products of the LANDFIRE project, *Int. J. Wildland Fire*, *18*, 250–267, doi:10.1071/WF08086.

Reid, J. S., R. Koppmann, T. F. Eck, and D. P. Eleuterio (2005), A review of biomass burning emissions part II: intensive physical properties of biomass burning particles, *Atmos. Chem. Phys.*, *5*, 799–825, doi:10.5194/acp-5-799-2005.

Reid, J. S., et al. (2009), Global monitoring and forecasting of biomass-burning smoke: Description of and lessons from the Fire Locating and Modeling of Burning Emissions (FLAMBE) Program, *IEEE J. Sel. Top. Appl. Earth Obs. Remote Sens.*, *2*(3), 144–162, doi:10.1109/JSTARS.2009.2027443.

Reinhardt, E. D., R. E. Keane, and J. K. Brown (1997), First Order Fire Effects Model: FOFEM 4.0, user's guide, *Gen. Tech. Rep. INT-GTR-344*, U.S. For. Serv., U.S. Dep. of Agric., Washington, D. C.

Riccardi, C. L., S. J. Pritchard, D. V. Sandberg, and R. D. Ottmar (2007a), Quantifying physical characteristics of wildland fuels using the Fuel Characteristic Classification System, *Can. J. For. Res.*, *37*, 2413–2420, doi:10.1139/X07-175.

Riccardi, C. L., R. D. Ottmar, D. V. Sandberg, A. Andreu, E. Elman, K. Kopper, and J. Long (2007b), The fuelbed: A key element of the Fuel Characteristic Classification System, *Can. J. For. Res.*, *37*, 2394–2412, doi:10.1139/X07-143.

Rolph, G. D., et al. (2009), Description and verification of the NOAA Smoke Forecasting System: The 2007 fire season, *Weather Forecast.*, *24*, 361–378, doi:10.1175/2008WAF2222165.1.

Schroeder, W., E. Prins, L. Giglio, I. Csiszar, C. Schmidt, J. Morisette, and D. C. Morton (2008), Validation of GOES and MODIS active fire detection products using ASTER and ETM plus data, *Remote Sens. Environ.*, *112*, 2711–2726, doi:10.1016/j.rse.2008.01.005.

Schultz, M. G., A. Heil, J. J. Hoelzemann, A. Spessa, K. Thonicke, J. G. Goldammer, A. C. Held, J. M. C. Pereira, and M. van het Bolscher (2008), Global wildland fire emissions from 1960 to 2000, *Global Biogeochem. Cycles*, *22*, GB2002, doi:10.1029/2007GB003031.

Seiler, W., and P. J. Crutzen (1980), Estimates of gross and net fluxes of carbon between the biosphere and atmosphere from biomass burning, *Clim. Change*, *2*, 207–247, doi:10.1007/BF00137988.

Shetler, G., M. R. Turetsky, E. Kane, and E. Kasischke (2008), Sphagnum mosses limit total carbon consumption during fire in Alaskan black spruce forests, *Can. J. For. Res.*, *38*, 2328–2336, doi:10.1139/X08-057.

Sikkink, P., and R. E. Keane (2008), A comparison of five sampling techniques to estimate surface fuel loading in montane forests, *Int. J. Wildland Fire*, *17*, 363–379, doi:10.1071/WF07003.

Simon, M., S. Plummer, F. Fierens, J. J. Hoelzemann, and O. Arino (2004), Burnt area detection at global scale using ATSR-2: The GLOBSCAR products and their qualification, *J. Geophys. Res.*, *109*, D14S02, doi:10.1029/2003JD003622.

Sitch, S., et al. (2003), Evaluation of ecosystem dynamics, plant geography and terrestrial carbon cycling in the LPJ dynamic global vegetation model, *Global Change Biol.*, *9*, 161–185, doi:10.1046/j.1365-2486.2003.00569.x.

Stocks, B. J., et al. (2003), Large forest fires in Canada, 1959–1997, *J. Geophys. Res.*, *108*(D1), 8149, doi:10.1029/2001JD000484.

Turetsky, M. R., and R. K. Wieder (2001), A direct approach to quantifying organic matter loss as a result of peatland wildfire, *Can. J. For. Res.*, *31*, 363–366, doi:10.1139/cjfr-31-2-363.

Turetsky, M., K. Wieder, L. Halsey, and D. Vitt (2002), Current disturbance and the diminishing peatland carbon sink, *Geophys. Res. Lett.*, *29*(11), 1526, doi:10.1029/2001GL014000.

Turetsky, M. R., E. S. Kane, J. W. Harden, R. D. Ottmar, K. L. Manies, E. Hoy, and E. S. Kasischke (2011), Recent acceleration of biomass burning and carbon losses in Alaskan forests and peatlands, *Nat. Geosci.*, *4*, 27–31, doi:10.1038/ngeo1027.

U.S. Forest Service (2007), Forest inventory and analysis strategic plan: A history of success; A dynamic future, *Rep. FS-865*, 20 pp., U.S. Dep. of Agriculture, Washington, D. C. (Available at http://fia.fs.fed.us/library/fact-sheets/overview/FIA_Strategic_Plan2.pdf.)

van der Werf, G., J. T. Randerson, L. Giglio, G. J. Collatz, P. S. Kasibhatla, and A. F. Arellano (2006), Interannual variability of global biomass burning emissions from 1997 to 2004, *Atmos. Chem. Phys.*, *6*, 3423–3441, doi:10.5194/acp-6-3423-2006.

van der Werf, G. R., J. T. Randerson, L. Giglio, G. J. Collatz, M. Mu, P. S. Kasibhatla, D. C. Morton, R. S. DeFries, Y. Jin, and T. T. van Leeuwen (2010), Global fire emissions and the contribution of deforestation, savanna, forest, agricultural, and peat fires (1997–2009), *Atmos. Chem. Phys. Discuss.*, *10*, 16,153–16,230, doi:10.5194/acpd-10-16153-2010.

Westerling, A. L., H. G. Hidalgo, D. R. Cayan, and T. W. Swetnam (2006), Warming and Earlier Spring Increase Western U.S. Forest Wildfire Activity, *Science*, *313*(5789), 940–943, doi:10.1126/science.1128834.

Wiedinmyer, C., B. Quayle, C. Geron, A. Belote, D. McKenzie, X. Zhang, S. O'Neill, and K. K. Wynne (2006), Estimating emissions from fires in North America for air quality modeling, *Atmos. Environ.*, *40*(19), 3419–3432, doi:10.1016/j.atmosenv.2006.02.010.

Wooster, M. J. (2002), Small-scale experimental testing of fire radiative energy for quantifying mass combusted in natural vegetation fires, *Geophys. Res. Lett.*, *29*(21), 2027, doi:10.1029/2002GL015487.

Wooster, M. J., G. Roberts, G. L. W. Perry, and Y. J. Kaufman (2005), Retrieval of biomass combustion rates and totals from fire radiative power observations: FRP derivation and calibration relationships between biomass consumption and fire radiative energy release, *J. Geophys. Res.*, *110*, D24311, doi:10.1029/2005JD006318.

Wright, C. S., R. D. Ottmar, and R. E. Vihnanek (2010), Critique of Sikkink and Keane's comparison of surface fuel sampling techniques, *Int. J. Wildland Fire*, *19*, 374–376, doi:10.1071/WF09084.

E. Alvarado, USFS PNW Fire and Environmental Research Team, Pacific Wildland Fire Sciences Laboratory, School of Forest Resources, University of Washington, 400 N 34th St., Ste. 201, Seattle, WA 98103, USA. (alvarado@u.washington.edu)

B. Amiro, Department of Soil Science, University of Manitoba, 364 Ellis Bldg., 13 Freedman Cresent, Winnipeg, MB R3T 2N2, Canada. (Brian_Amiro@umanitoba.ca)

W. J. de Groot, Great Lakes Forestry Research Centre, Canadian Forest Service, 1219 Queen St. East, Sault Ste Marie, ON P6A 2E5, Canada. (Bill.deGroot@NRCan-RNCan.gc.ca)

B. de Jong, El Colegio de la Frontera Sur, Unidad Villahermosa, Carretera a Reforma km 15.5 s/n; Ra Guineo 2da Secc, 86280, Villahermosa, Tabasco, México. (bjong@ecosur.mx)

N. H. F. French and L. K. Jenkins, Michigan Tech Research Institute, Michigan Technological University, 3600 Green Ct., Ste. 100, Ann Arbor, MI 48105, USA. (nancy.french@mtu.edu; liza.jenkins@mtu.edu)

S. Goetz, Woods Hole Research Center, 149 Woods Hole Rd., Falmouth, MA 02540, USA. (sgoetz@whrc.org)

E. Hoy, Department of Geography, University of Maryland, 2181 LeFrak Hall, College Park, MD 20742, USA. (ehoy@umd.edu)

E. Hyer, Marine Meteorology Division, Naval Research Laboratory, 7 Grace Hopper Ave., Monterey, CA 93943, USA. (edward.hyer@nrlmry.navy.mil)

R. Keane, Missoula Fire Sciences Laboratory, U.S. Forest Service, 5775 West US Hwy. 10, Missoula, MT 59808-9361, USA. (rkeane@fs.fed.us)

B. E. Law, College of Forestry, Oregon State University, 328 Richardson Hall, Corvallis, OR 97331, USA. (bev.law@oregonstate.edu)

D. McKenzie and R. Ottmar, Pacific Wildland Fire Sciences Laboratory, U.S. Forest Service, 400 N 34th St., Ste. 201, Seattle, WA 98103, USA. (donaldmckenzie@fs.fed.us; rottmar@fs.fed.us)

S. G. McNulty, Eastern Forest Environmental Threat Assessment Center, U.S. Forest Service, Southern Research Station, 920 Main Campus Dr., Ste. 300, Raleigh, NC 27606, USA. (steve_mcnulty@ncsu.edu)

D. R. Pérez-Salicrup, Centro de Investigaciones en Ecosistemas, Universidad Nacional Autónoma de México, Antigua Carretera a Pátzcuaro 8701, Morelia, Michoacán, CP 58190, México. (diego@oikos.unam.mx)

J. Randerson and B. M. Rogers, Earth System Science Department, University of California, 3242 Croul Hall, Irvine, CA 92697-3100, USA. (jranders@uci.edu; bmrogers@uci.edu)

K. M. Robertson, Tall Timbers Research Station, 13093 Henry Beadel Dr., Tallahassee, FL 32312, USA. (krobertson@ttrs.org)

M. Turetsky, Department of Integrative Biology, University of Guelph, Guelph, ON N1G 1G2, Canada. (mrt@uoguelph.ca)